Article

Current Biology

Ancient Bacterial Genomes Reveal a High Diversity of *Treponema pallidum* Strains in Early Modern Europe

Graphical Abstract

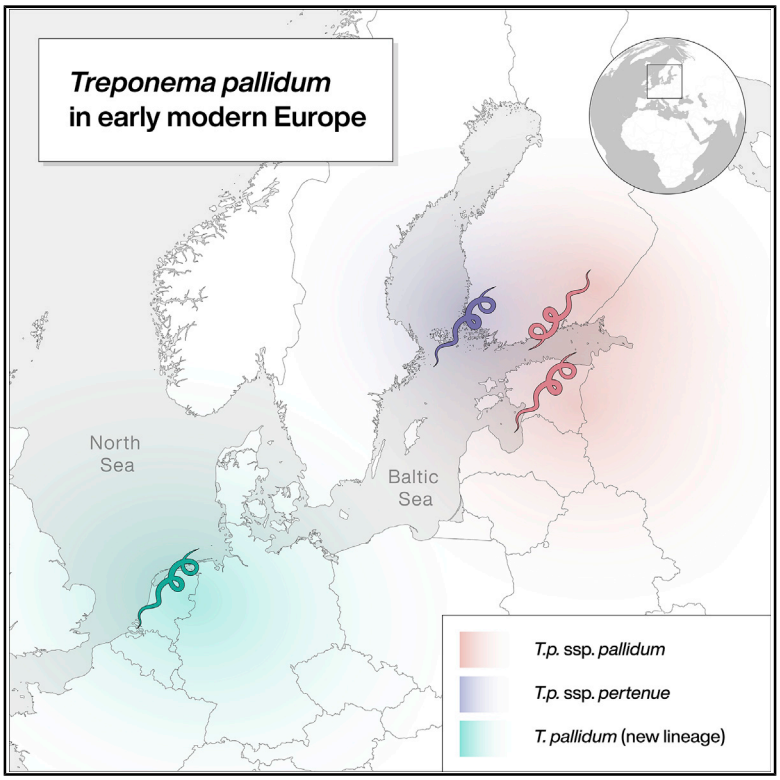

Highlights

- Four ancient *Treponema pallidum* genomes from early modern Europe were reconstructed
- The genomes are highly diverse and include syphilis, yaws, and an unknown lineage
- The new ancient *T. pallidum* lineage is a basal sister group to yaws and bejel
- Molecular clock dating would allow a pre-Columbian origin of *T. pallidum* in Europe

Authors

Kerttu Majander, Saskia Pfrengle, Arthur Kocher, ..., Denise Kühnert, Johannes Krause, Verena J. Schuenemann

Correspondence

kerttu.majander@uzh.ch (K.M.), krause@shh.mpg.de (J.K.), verena.schuenemann@iem.uzh.ch (V.J.S.)

In Brief

Majander et al. find a high diversity among the first ancient European treponemal genomes, including a newly discovered lineage. Dated around Columbus' contact with the Americas, these lineages and their overlapping spatial distributions suggest a possible Old-World origin of syphilis and the existence of endemic treponematoses in Europe.

Majander et al., 2020, Current Biology *30*, 3788–3803
October 5, 2020
https://doi.org/10.1016/j.cub.2020.07.058

CellPress

CellPress
OPEN ACCESS

Current Biology

Article

Ancient Bacterial Genomes Reveal a High Diversity of *Treponema pallidum* Strains in Early Modern Europe

Kerttu Majander,[1,2,3,4,18,*] Saskia Pfrengle,[1,2,18] Arthur Kocher,[5] Judith Neukamm,[1,2,6] Louis du Plessis,[7] Marta Pla-Díaz,[8,16] Natasha Arora,[9] Gülfirde Akgül,[1] Kati Salo,[4,10] Rachel Schats,[11] Sarah Inskip,[12] Markku Oinonen,[13] Heiki Valk,[14] Martin Malve,[14] Aivar Kriiska,[14] Päivi Onkamo,[4,15] Fernando González-Candelas,[8,16] Denise Kühnert,[5] Johannes Krause,[2,3,17,*] and Verena J. Schuenemann[1,2,17,19,*]

[1]Institute of Evolutionary Medicine, University of Zurich, Winterthurerstrasse 190, 8057 Zurich, Switzerland
[2]Institute for Archaeological Sciences, University of Tübingen, Rümelinstrasse 19-23, 72070 Tübingen, Germany
[3]Department of Archaeogenetics, Max Planck Institute for the Science of Human History, Kahlaische Strasse 10, 07745 Jena, Germany
[4]Department of Biosciences, University of Helsinki, Viikinkaari 9, 00014 Helsinki, Finland
[5]Transmission, Infection, Diversification and Evolution Group, Max Planck Institute for the Science of Human History, Kahlaische Strasse 10, 07745 Jena, Germany
[6]Institute for Bioinformatics and Medical Informatics, University of Tübingen, Sand 14, 72076 Tübingen, Germany
[7]Department of Zoology, University of Oxford, Oxford OX1 3SZ, UK
[8]Joint Research Unit "Infection and Public Health" FISABIO-University of Valencia, Institute for Integrative Systems Biology (I2SysBio), Valencia, Spain
[9]Zurich Institute of Forensic Medicine, University of Zurich, Winterthurerstrasse 190/52, 8057 Zurich, Switzerland
[10]Archaeology, Faculty of Arts, University of Helsinki, Unioninkatu 38F, 00014 Helsinki, Finland
[11]Laboratory for Human Osteoarchaeology, Faculty of Archaeology, Leiden University, Einsteinweg 2, 2333CC Leiden, the Netherlands
[12]McDonald Institute for Archaeological Research, University of Cambridge, Downing Street, Cambridge CB2 3ER, UK
[13]Laboratory of Chronology, Finnish Museum of Natural History, University of Helsinki, Gustaf Hällströmin katu 2, 00560 Helsinki, Finland
[14]Institute of History and Archaeology, University of Tartu, Jakobi 2, 51005 Tartu, Tartumaa, Estonia
[15]Department of Biology, University of Turku, Vesilinnantie 5, 20500 Turku, Finland
[16]CIBER de Epidemiología y Salud Pública (CIBERESP), Madrid, Spain
[17]Senckenberg Centre for Human Evolution and Palaeoenvironment (S-HEP), University of Tübingen, Tübingen, Germany
[18]These authors contributed equally
[19]Lead Contact
*Correspondence: kerttu.majander@uzh.ch (K.M.), krause@shh.mpg.de (J.K.), verena.schuenemann@iem.uzh.ch (V.J.S.)
https://doi.org/10.1016/j.cub.2020.07.058

SUMMARY

Syphilis is a globally re-emerging disease, which has marked European history with a devastating epidemic at the end of the 15th century. Together with non-venereal treponemal diseases, like bejel and yaws, which are found today in subtropical and tropical regions, it currently poses a substantial health threat worldwide. The origins and spread of treponemal diseases remain unresolved, including syphilis' potential introduction into Europe from the Americas. Here, we present the first genetic data from archaeological human remains reflecting a high diversity of *Treponema pallidum* in early modern Europe. Our study demonstrates that a variety of strains related to both venereal syphilis and yaws-causing *T. pallidum* subspecies were already present in Northern Europe in the early modern period. We also discovered a previously unknown *T. pallidum* lineage recovered as a sister group to yaws- and bejel-causing lineages. These findings imply a more complex pattern of geographical distribution and etiology of early treponemal epidemics than previously understood.

INTRODUCTION

Treponemal infections, namely yaws, bejel, and, most notoriously, syphilis, represent a reoccurring, global threat to human health. Venereal syphilis, caused by infections with *Treponema pallidum pallidum* (TPA) results in millions of new cases every year [1]. The two endemic treponemal subspecies closely related to *T. p. pallidum* are *T. pallidum pertenue* (TPE) and *T. pallidum endemicum* (TEN). TPE is common in the tropical regions of the world, where it causes yaws and a non-human primates' treponematosis [2–4]. TEN is the causative agent of bejel, which is mostly found in hot and arid environments [2, 3]. All three *T. pallidum* subspecies are re-emerging across numerous countries, prompting renewed international eradication campaigns [5, 6]. Furthermore, resistance against second-line antibiotics has recently been observed for each of them [7–9], although penicillin treatment still remains effective [8, 10–12]. Yaws, bejel, and syphilis are all transmitted through direct contact with skin

lesions or mucous membranes [2, 3]. Syphilis is generally transmitted sexually or congenitally, although incidental transmission through other routes, such as blood transfusions, is occasionally observed [2, 3]. Contrarily, the endemic treponematoses (yaws and bejel) are most commonly transmitted through skin lesions, primarily in childhood or preadolescence [3, 13]. All three diseases overlap in clinical manifestations, with progression through multiple stages and damage to the skin and other tissues [14, 15]. The syphilis-causing bacterium (TPA) is considered highly invasive, disseminating through the body and into the central nervous system; if untreated, it can result in severe damage to organs and tissues, including the skeletal system [3, 14–16].

The re-emergence of treponemal diseases after the devastating outbreaks documented in historical times showcases a spread facilitated by pathogen evolution in combination with social factors [8, 12, 17–19]. Early medical reports from the late 15th century portray the most well-known epidemic, a rapid and Europe-wide spread of venereal syphilis in the wake of the 1495 Italian war [17, 20], whereas reports from later periods appear to indicate a gradual shift to a milder, more chronic disease in the subsequent decades, similar in manifestation to modern-day syphilis [17, 21, 22]. The European outbreak coincides with the first American expeditions and has ignited a persisting theory suggesting that syphilis was introduced to Europe by Columbus and his crew upon their return from the New World in 1493 [23, 24]. The alternative multiregional hypothesis contradicts this scenario and presumes the pre-Columbian presence of syphilis on the European continent, potentially as a result of prehistoric spread of the disease through African and Asian routes [25–27]. Medieval literature mentions cases of syphilis, but it is often diagnostically confounded by similarities with other diseases and spuriously called ‘‘venereal’’ or ‘‘hereditary’’ leprosy [22, 28]. Pre-Columbian human remains with characteristic marks of treponematoses have been reported [29, 30] yet are thus far unconfirmed with genetic evidence [23, 28]. Distinguishing the *T. pallidum* infections from other diseases is often challenging [31], and although serological tests allow diagnosing them, more precise distinction among treponemal subspecies requires molecular typing [15, 32, 33]. Before modern genetic classifications were introduced, supporters of the ‘‘unitarian hypothesis’’ claimed all treponematoses to be one and the same disease [34, 35]. Improved understanding of phylogenetic cladality among the treponemal subspecies [36, 37], further refined by genomic studies, has since disputed the unitarian view [3, 38, 39]. Questioning the geographical distribution and clinical symptoms as the main means of categorization can, nevertheless, be justified, as the geographical origin and time of emergence of TPA and TPE remain ambiguous [17, 40, 41]. A recent genomic study on modern lineages of *T. pallidum* supported a common ancestor of all current TPA strains in the 1700s [41], whereas the more general diversification of *T. pallidum* into subspecies is assumed to have happened in prehistoric times [24, 42]. However, mutation rate estimates drawn from modern genome isolates may be biased, because natural selection has not affected the most recent mutations yet [43] and large parts of the past species diversity may have been lost in time [44]. Reconstructed ancient pathogen genomes thus show an unprecedented potential to illuminate their species’ unresolved divergence times, origin, and evolution [45–47]. Ancient DNA studies on treponematoses have so far remained scarce for both biological and methodological reasons. The treponemal spirochetes survive poorly outside their host organism and are present in extremely low quantities during late-stage infections, often evading detection even in living patients [48]. The final, tertiary-stage treponematoses produce the most frequently detected skeletal alterations, but in these cases, the disease has often already reached the latent stage, thwarting attempts to retrieve its DNA [49, 50]. Most notably, the bones most likely containing large amounts of treponemal agents belong to congenitally infected neonates. Such finds, however, are very rare in the archaeological record [51, 52]. Currently, technical advancements, together with careful selection of samples exhibiting signs of treponemal pathogenesis, are enabling genomic studies on this elusive pathogen for the first time [53]. The means to recover *T. pallidum* from historic human remains were recently established in a study on perinatal and infant individuals from colonial Mexico, in which two ancient *T. p. pallidum* genomes and one ancient *T. p. pertenue* genome were described [52]. Attempts to retrieve authentic *T. pallidum* DNA from ancient adult individuals have so far been unsuccessful.

Here, we analyze ancient bacterial genomes from four ancient *T. pallidum* strains retrieved with target enrichment from subadult and adult human remains originating from central and northern Europe. The newly reconstructed ancient genomes represent a variety of *T. pallidum* subspecies, including a formerly unknown form of treponematosis phylogenetically basal to both bejel- and yaws-causing lineages. For the first time, treponemal genomes dated temporally close to New World contact have been retrieved from European samples, including strains closely related to *T. pallidum* subspecies that are today mostly restricted to the tropics and subtropics.

RESULTS

Geographical Origins and Osteological Analyses of Samples

For this study, remains from nine individuals were included: five from the Holy Ghost Chapel in Turku, Finland; one from the Dome churchyard in Porvoo, Finland; one each from St. Jacob’s cemetery and from St. George’s cemetery in Tartu, Estonia; and, finally, one from Gertrude’s Infirmary in Kampen, the Netherlands (STAR Methods). Four samples from these individuals tested positive for treponemal infection in the DNA screening with high-throughput sequencing (Figure 1A). The sampled premolar CHS119 (Figure 1A1) is from an adult individual from Turku with several treponemal changes on the skull and both tibias [54]. The petrous bone sample PD28 from Porvoo (Figure 1A2) showed no syphilis-associated lesions [55]; an infection was implicated primarily by the individual’s perinatal death. The skeleton of a young adult from Tartu (Figure 1A3) yielding the sample SJ219 displayed putative albeit inconclusive indicators of syphilis. From the adolescent individual from Kampen, only a disarticulated tibia was available [24] with an active lesion on the cortical surface, which was used to obtain sample KM14-7 (Figure 1A4).

All four positive samples in this study were radiocarbon dated (STAR Methods). The putatively pre-Columbian samples

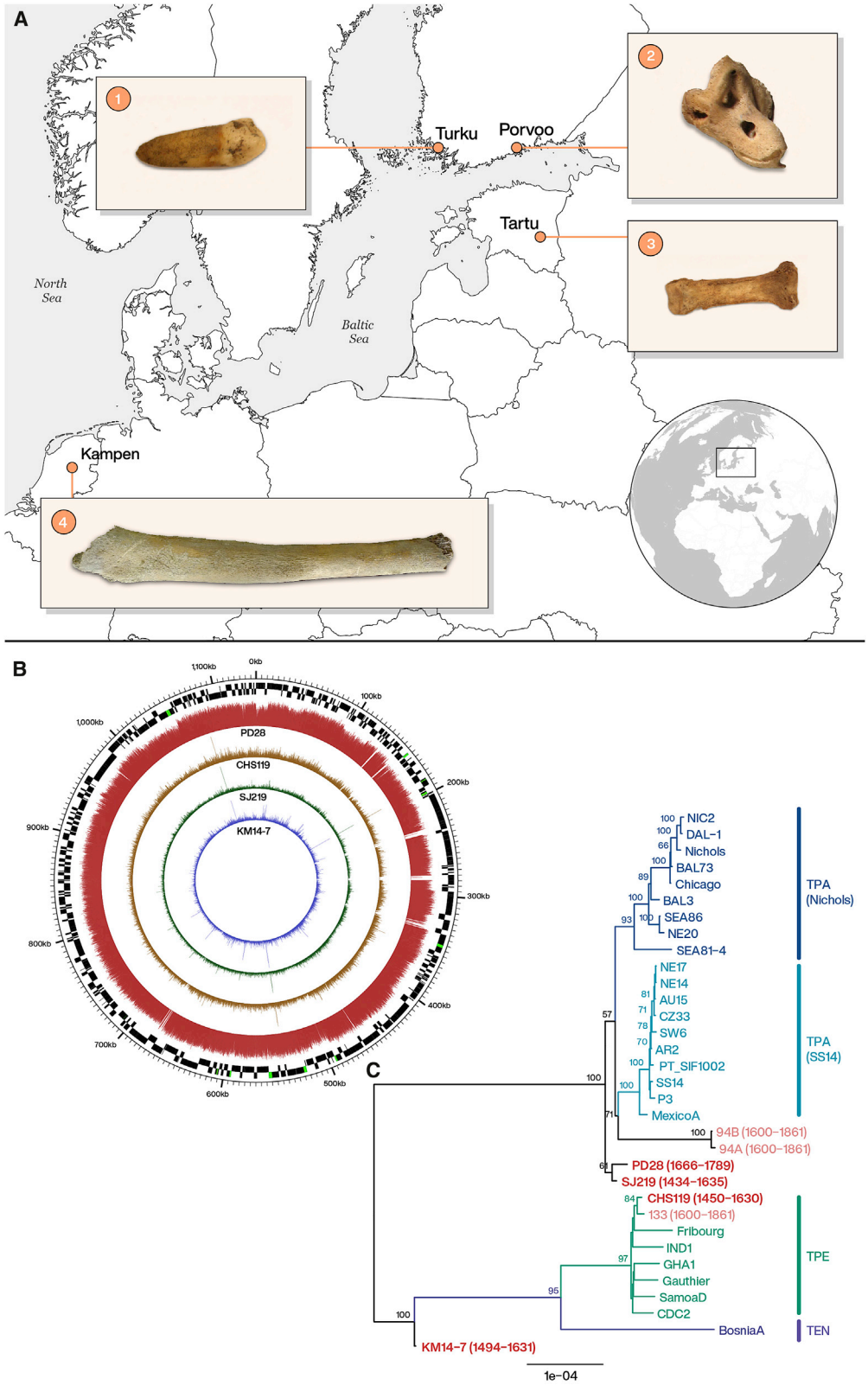

Figure 1. Geographical Origin and Phylogenetic Placement of *T. pallidum*-Positive Samples

(A) Locations of archeological sites from which the samples used in this study originate: (1) a premolar from an adult individual 119, crypt of the Holy Ghost Chapel, Turku, Finland; (2) petrous portion of temporal bone of a perinatal individual from the grave 28 at the Porvoo Dome cemetery, Porvoo, Finland; (3) a proximal

(legend continued on next page)

CHS119 and SJ219 went through additional attestation of the dating procedures: a fragment of the wooden platform from the grave was dated in addition to the individual SJ219, and reservoir effect corrections were calculated for the sample CHS119 dating results [57, 58]. These additional estimates, however, resulted in upper limit date ranges within the 17th century CE for both individuals (STAR Methods).

Authenticity Estimation of Ancient DNA and Genome Reconstruction

All samples included in this study (Table 1; STAR Methods) were subjected to a screening procedure using direct shotgun sequencing and genome-wide enrichment [41, 59]. In this screening, samples yielding a minimum 1,000 post-duplicate-removal reads mapping to a *T. pallidum* reference (SJ219: 1,205 reads; CHS119: 1,496 reads; KM14-7: 1,496 reads; PD28: 1,637 reads) were deemed positive for this pathogen (for damage profiles, see Figure S2). The percentage of deaminated bases at the ends of reads, signaling authenticity of ancient DNA [60, 61], ranged from 4% to 18% (*T. pallidum* DNA; screening capture) and 10% to 18% (mitochondrial DNA [mtDNA]; mitochondrial capture), and the average fragment length of the four samples varied between 49 and 69 bases (Table 1). An array capture enrichment for *T. pallidum* DNA [41, 59] using uracil-DNA glycosylase (UDG)-treated libraries [62] was then conducted on all four positive samples, and additionally, human mtDNA was enriched for samples CHS119, SJ219, and KM14-7 [59, 63] (STAR Methods). The mtDNA ranged from 3,414 to 29,031 mapped reads, with an average coverage of 11–119× on the mitochondrial genome (Table 1). Haplogroups identified were J1c2c1 for CHS119, HV16 for SJ219, and U2e1f1 for KM14-7 (Table 1), all representative of the early modern variation present within northern and central European populations, further supporting the geographical origin of the samples [64, 65].

After high-throughput sequencing of the enriched DNA on Illumina platforms, the resulting 98–256 million raw reads were merged sample-wise and duplicate reads were removed. Genomes for each sample were reconstructed by mapping to the *T. p. pallidum* reference genome Nichols (CP004010.2), using the EAGER pipeline [69] (STAR Methods). The samples yielded between 18,034 and 1,430,292 endogenous unique reads mapping to the reference, covering 47%–98% of the reference genome at least once, respectively (Table 1; Figures 1B and S3). We filtered positions based on read coverage and excluded recombining and other potentially mapping-obstructing genes (*FadL* homologs, *tpr* genes, and *arp* gene), as well as the genomic positions for which >25% of the genomes had missing data, gaining complete genome alignments containing a total of 1,631 variable positions. We refer to these positions as single nucleotide polymorphisms (SNPs) throughout the manuscript.

Phylogenetic Analysis and Genetic Recombination

Midpoint-rooted maximum-likelihood (ML) trees of our ancient European genomes, previously published colonial Mexican genomes [52], and 26 modern treponemal genomes [41, 70–78] were reconstructed from the alignments. The four ancient European genomes are placed at three distinct positions in the phylogenetic tree (Figures 1C and 2). The PD28 and SJ219 genomes most closely resemble syphilis-causing strains and form a sister group to all other TPA strains, although this position is not highly supported and seems highly sensitive to the set of genes excluded from the alignment (Figure S4). The CHS119 genome, conversely, is consistently placed in the TPE clade of the treponemal family tree and forms a cherry with the ancient TPE genome 133 from colonial Mexico. The affinity of these two ancient genomes may in part result from similarly missing data with respect to the complete genomes of modern strains in the clade. The KM14-7 genome, remarkably, falls basal to all TPE lineages known today, as well as to the TEN genome Bosnia A [76]. This unexpected position was further corroborated by investigating genomic loci for which the ancestral variants of the TPE/TEN and TPA clades were likely different. Among 30 of these positions for which the variant was resolved in KM14-17, 60% were TPE/TEN-like and 40% were TPA-like, which supports the branching of this genome on the evolutionary path between TPA and TPE/TEN clades. In comparison, all other genomes had 100% variant characteristics of one or the other clade at these positions, except for 94A, 94B, and SEA81-4, which had 16%, 14.3%, and 10.7% of TPE/TEN-like variants, respectively (Tables S1 and S2). The basal position of KM14-7 retained strong support also when using an alignment including only nucleotide positions resolved in this genome (Figure S4F) or using an alternative alignment based on mapping to the TPE CDC2 reference genome (Figures 2B and 2C), thus disputing the possibility that its phylogenetic placement would be an artifact of missing data or dependent on a specific reference genome.

A recombination analysis was conducted as described in Arora and colleagues [41], including 26 modern genomes [41, 70–78] and six ancient ones: the colonial Mexican genomes 94A, 94B, and 133 from an earlier study [52] and three of our ancient European genomes, namely PD28, CHS119, and SJ219 (Table 2). Sample KM14-7 was excluded from the analysis, due to its sporadic placement in the ML tree topologies,

manual phalanx of a young adult individual from St. Jacob's cemetery, Tartu, Estonia; and (4) a tibia from a subadult individual from Gertrude's Infirmary, Kampen, the Netherlands.

(B) Circleator [56] plot representing the entire data from the respective BAM files after duplicate removal and mapped with a quality threshold 37, showing the coverage of the four ancient strains. The genome coverage of the ancient strains is shown from lowest to highest: KM14-7; SJ219; CHS119; and PD28, with colors from inside to outside in violet, green, brown, and red. As setting the quality threshold above zero allows no reads mapping to identical sequences, gaps in coverage occur in each of the genomes on the identical regions. The black outer rim visualizes the protein-coding regions in forward and the black inner rim in the reverse direction, according to the annotation of the Nichols reference genome (CP004010.2).

(C) Midpoint-rooted maximum-likelihood phylogenetic tree of *Treponema pallidum* strains. The analysis is based on an alignment of 1,631 SNPs after exclusion of recombining and hypervariable genes as well as genomic positions with >25% missing data. Branch lengths represent numbers of substitutions per site. Bootstrap support values are written above nodes when >50. Ancient genomes from this study are marked in red and the previously published ones in pink. See also Figures S3 and S4.

Table 1. Mapping Statistics

Data Type	Ind. ID	Arch. ID	Mol. Sex (from Shotgun Data)	Raw Reads	Mapped Reads (Post-duplicate Removal)	AVG Cov.	% Gen. Cov. 1×	% Gen. Cov. 2×	% Gen. Cov. 3×	% Gen. Cov. 5×	DNA Dmg 1st Base 5′ (Non-UDG)	AVG Frag. Length	Cont. Est.	Haplo-group
TP	PD28	grave 28	XY	98,204,923	1,430,292	136.23	98.09	98.07	98.06	98.04	0.04	59.91	N/A	N/A
MT					N/A	N/A	N/A	N/A	N/A	N/A	N/A	N/A	N/A	N/A
TP	SJ219	individual 219	XX	193,609,543	29,198	1.41	64.31	34.00	15.69	2.58	0.10	49.12	N/A	N/A
MT					29,031	118.91	100	100	100	100	0.13	67.74	0.02	HV16
TP	CHS119	individual 119	XX	255,889,929	52,054	2.82	83.32	62.31	42.04	15.13	0.18	54.16	N/A	N/A
MT					4,490	16.25	100	100	99.99	99.79	0.14	59.85	0.02	J1c2c1
TP	KM14-7	individual 14, bone fragment 7	XY	152,268,578	18,034	0.91	46.89	19.35	7.93	1.61	0.18	51.69	N/A	N/A
MT					3,414	11.02	99.98	99.77	99.37	96.08	0.16	53.35	0.01	U2e1f1

Statistics from the EAGER pipeline against the Nichols reference genome for the four ancient samples screened as positive for treponemal infection. The individual (Ind) and original archaeological (Arch.) identifiers are reported for each sample. The table includes final number of raw reads; mapped reads after duplicate removal; average coverage (AVG cov.); percent of the genome covered at 1-fold, 2-fold, 3-fold, and 5-fold coverage; percent of reads with DNA damage (DNA dmg) for the 1st base at the 5′ end (non-UDG treated); and average fragment length (AVG frag. length) in base pairs for the treponemal and *T. pallidum* (TP) capture data. Same statistics are given for the human mitochondrial capture data (MT) where applicable, with the addition of an estimated amount of contamination (Cont. est.) from Schmutzi program [66] and haplogroup assignments from HaploGrep2 [64] program. Molecular sexing (Mol. sex) of individuals is based on the human endogenous reads from shotgun data [67, 68].

which were derived for entire genomes and for each gene individually. Congruence between the complete genome alignments and gene trees was tested after evaluating the corresponding phylogenetic signal for each gene. The phylogenetic signal and incongruence proved significant for 40 loci, twelve of which were further verified by the presence of at least three consecutive SNPs supporting a recombination event. A total of 316 SNPs was identified in 16 recombinant regions in 12 different genes. Two of the recombining gene candidates identified by Arora and colleagues [41] were also confirmed in association with the ancient European genomes. Among our ancient genomes, PD28 (along with the Nichols clade) was possibly involved in one recombinant event of the TP0136 gene as a putative recipient, with the TPE/TEN clade, CHS119, and colonial Mexican 133 genomes as putative donors. Similar possibility was observed in the recombination event detected in the TP0179 gene, although only with TPE/TEN clade and 133 as presumptive donors. One putative recombination event concerning the TP0865 gene was identified between the CHS119 and 133 genomes (along with the TPE/TEN clade) and the SEA86, NE20, and SEA81-4 lineages. Finally, another recombination event concerned the TP0558 gene, with the TPE/TEN clade and CHS119 genome as potential donors and the SS14 clade, MexicoA, 94A, and 94B from colonial Mexico and PD28 genomes as recipients. The events observed between the modern strains and including the previously published colonial Mexican genomes are listed in Table 2.

Molecular Clock Dating

Molecular clock dating analyses were performed on a dataset of 28 genomes [41, 70–78] (STAR Methods). Linear regression of root-to-tip genetic distance against sampling date indicated that the *T. pallidum* strains possess a good temporal signal ($r = 0.66$; $p < 0.001$; Figures S5A–S5C; STAR Methods).

The date randomization test (DRT) [81] showed that neither the mean nor median estimate of the clock rate estimated under the true sampling dates was contained within the highest posterior density (HPD) intervals of estimates from any of the replicates with permuted sampling dates (Figure S5D). Furthermore, the HPD intervals of only 1 out of 50 replicates intersect with the HPD interval estimated under the true sampling dates. We interpret these results as evidence of a substantially stronger molecular clock signal in the dataset than is expected by chance. Finally, robustness analyses with different combinations of demographic and clock models showed that the demographic model has little effect on the estimated divergence times and sampling dates and that a relaxed clock model receives strong support (Figure S6).

Posterior distributions of divergence dates of *T. pallidum* clades and sampling dates of ancient genomes are shown in Figure 3A. Figure 3B shows the maximum clade credibility (MCC) tree estimated in BEAST2 v.2.6 [82]. Sampling date estimates under different models are given in Figures S6I–S6L and Table 3. The time to the most recent common ancestor (T_{MRCA}) calculated for the whole *T. pallidum* family is placed far in the prehistoric era, at least 2000 BCE. However, time dependency of molecular rates (TDMR) may lead to underestimating deep divergence times when mutation rates are inferred from genomes collected within a relatively restricted time period [83, 84]. Applying a model accounting for TDMR may be possible in the

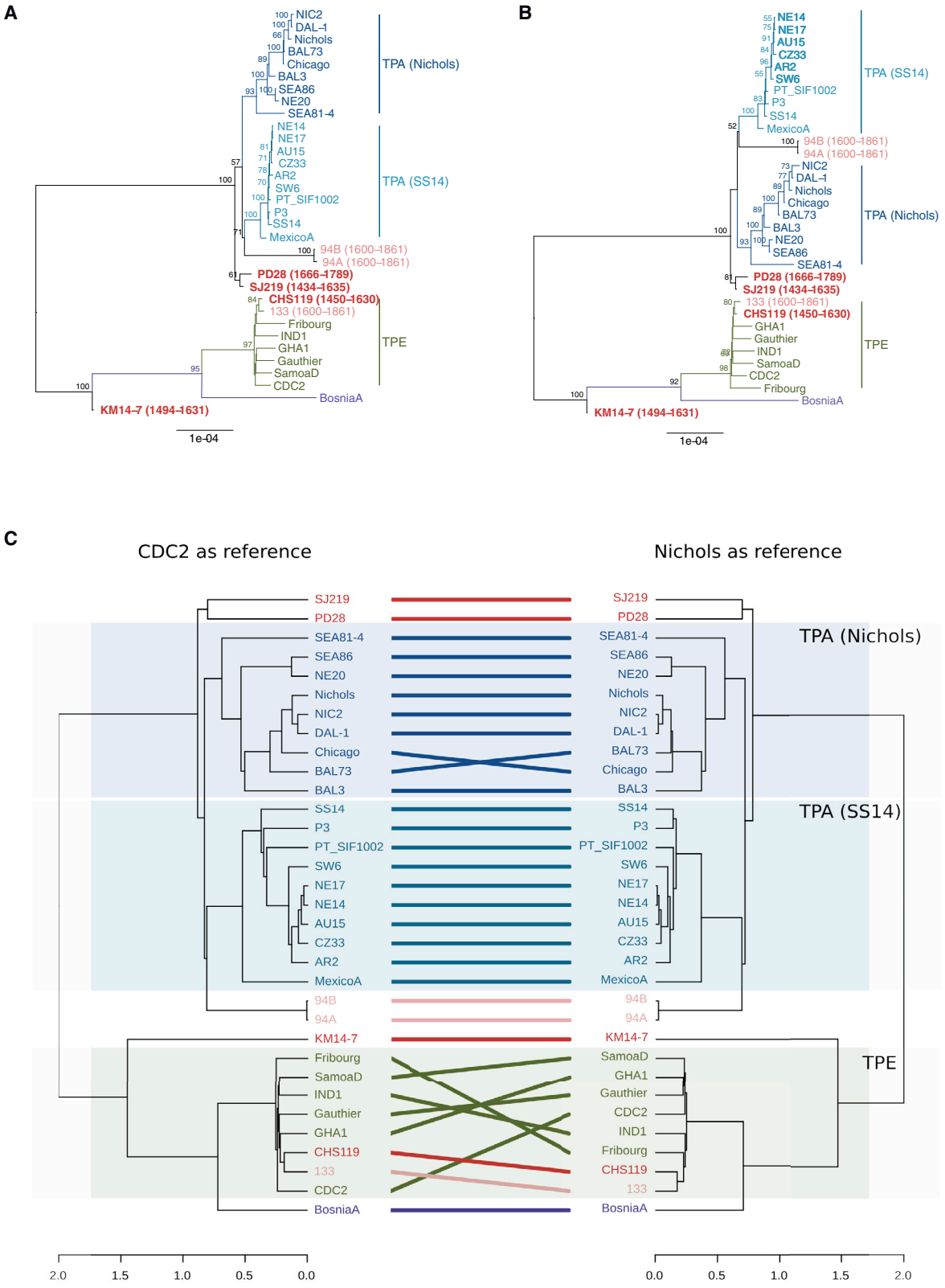

(legend on next page)

Table 2. Recombination Events

Gene ID	Event	Start	End	Minimal Size	Strains Involved
TPANIC_0136	3	158,271	158,336	65	yaws → Nichols clade
	4	158,346	158,364	18	yaws/Bosnia A → Nichols clade
	5	158,915	158,976	61	yaws/Bosnia A/133/CHS119? → PD28, Nichols clade[a]
	6	159,312	159,323	11	yaws/Bosnia A/133 → Nichols clade
TPANIC_0164	1	187,064	187,177	113	yaws/Bosnia A → Sea86, NE20, 94A, 94B
TPANIC_0179	1	198,040	198,428	388	yaws/Bosnia A/133 → PD28, Nichols clade[a]
TPANIC_0326	1	345,859	347,956	2,097	Bosnia A → SS14 clade
TPANIC_0462	1	492,772	493,605	833	yaws/Bosnia A → Sea86, NE20
TPANIC_0488	1	522,981	523,620	639	Bosnia A → Mexico A
TPANIC_0515	1	555,872	557,768	1,896	yaws/Bosnia A/133 → 94A, 94B, Nichols clade
TPANIC_0548	1	593,563	594,215	652	yaws/Bosnia A → Nichols clade
TPANIC_0558	1	606,171	606,591	420	yaws/Bosnia A/CHS119?/133? → PD28, 94B, 94A? SS14 clade, Mexico A[a]
TPANIC_0865	1	945,224	945,542	318	yaws/Bosnia A/CHS119?/133? → Sea86, NE20, Sea81-4[a]
	2	945,830	946,298	468	Bosnia A → Sea86, NE20, Sea81-4
TPANIC_0967	1	1,051,257	1,052,366	1,109	yaws/Bosnia A → Sea81-4
TPANIC_0968	1	1,052,414	1,053,617	1,203	Bosnia A → Sea81-4

All detected recombination events across the complete dataset of 26 modern *Treponema pallidum* [41, 70–78] and six ancient genomes (94A, 94B, and 133 from [52] and genomes PD28, CHS119, and SJ219 from this study). For each recombination event are reported the start and end position of the event referred to as TPA Nichols strain, accession CP004010.2. Slashes are used to separate the different potential gene donor strains. The affected recipient strains are separated by commas. Arrows point to the likely direction of recombination between the donor and recipient strains. An interrogation mark indicates an uncertain yet likely involvement in the event.
[a]Events involving ancient genomes from this study

future, if genomes covering wider and more distinct time periods become available [85, 86]. The latest common ancestor of the venereal syphilis strains was placed between the 12th and 16th centuries CE. The divergence of TPE and TEN was dated to between the 4th century BCE and the 12th century CE, although the most recent common ancestor of TPE was placed between the 14th and 16th centuries CE. The best supported tree topology places the ancient European genomes basal to all TPA strains, with the T_{MRCA} of the modern Nichols clade between the 15th and 18th centuries CE and that of the SS14 clade slightly later, between the 18th and 20th centuries CE. Due to the inclusion of four ancient European genomes, the above divergence times are substantially older than the times reported by Arora and colleagues [41]. Similarly, the estimated mean molecular clock rate (1.069×10^{-7} s/s/y; 95% HPD $7.277 \times 10^{-8} - 1.516 \times 10^{-7}$ s/s/y) is slower than those reported in recent studies [8, 41] for either *T. pallidum* as a whole or for TPA strains exclusively. Nonetheless, the 95% HPD of the mean clock rate overlaps with previous estimates [8] (Figure S6A).

Molecular clock dating allows us to refine the sampling date estimates for three of the four ancient genomes (Figure 3A). The posterior distribution of the sampling date of CHS119 places most of the weight on a more recent date, although those of PD28 and 133 favor older sampling dates. This is especially pronounced for CHS119 and 133 with the 95% HPD interval not including any dates older than 1546 CE for CHS119 or younger than 1782 CE for 133. On the other hand, for SJ219, the 95% HPD of the sampling date spans nearly the entire range defined by radiocarbon dating, making it impossible to exclude a pre-Columbian sampling date (posterior probability 0.28; Table 3).

Virulence Factor Analysis

A set of 60 TPA candidate genes associated with virulence and outlined in previous studies [52, 87, 88] were queried in the ancient European samples to determine their presence or absence and thus to broadly assess the extent of functional changes between ancient and modern treponemal lineages. A color-coded heatmap was produced to visualize the percentage of coverage on these 60 candidate genes for each genome (Figure 4). These selected genes included the family of *tpr* genes, which mostly encode putative outer membrane proteins. The *tpr* genes are grouped into three subfamilies of paralogous genes and pose challenges to their distinction with short read data due to high sequence homology. Given that mapping and filtering parameters with a MAPQ score threshold above 0 results in the exclusion of reads mapping to more than one location, and therefore in lower genetic coverage, MAPQ score thresholds of

Figure 2. Phylogenies Comparing the Effect of Mapping to TPA (Nichols) and TPE (CDC2) Reference Genome

(A and B) A comparison of the phylogenetic ML trees based on SNP alignments after evaluation of precarious SNPs and removal of hypervariable and recombinant genes, when mapped against (A) *Treponema pallidum pallidum* reference genome Nichols (CP004010.2) and (B) *Treponema pallidum pertenue* reference genome CDC2 (CP002365.1). Scale bar represents substitutions per nucleotide site.

(C) Tanglegram visualization of the observed topological differences between the two mappings, produced using R packages ape [79] and dendextend [80]. Horizontal scales measure statistical similarity of the two trees in comparison to each other.

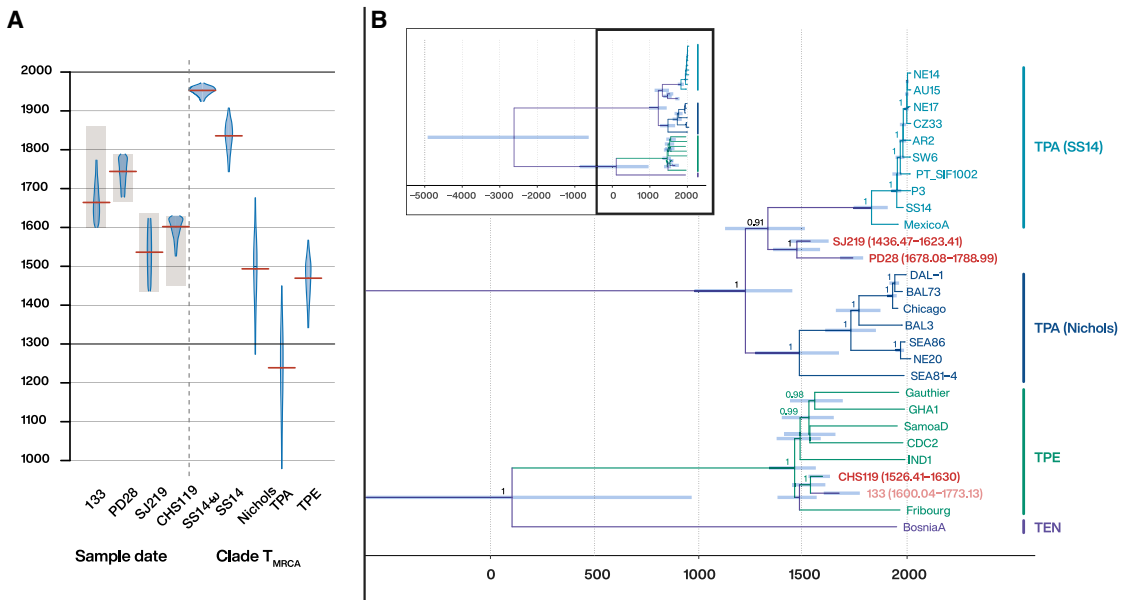

Figure 3. Molecular Clock Dating

(A) Posterior distributions for the sampling dates of ancient genomes (left) and the divergence dates of more recent clades in the tree (right). The distributions are truncated at the upper and lower limits of the 95% highest posterior density (HPD) intervals, and the red lines indicate the median estimates. The shading indicates the prior distributions used for the sampling dates of ancient samples (informed by radiocarbon date ranges). Vertical scale denotes time in years CE.

(B) Maximum clade credibility (MCC) tree of the dataset consisting of 24 modern and four ancient genomes estimated in BEAST2 v2.6 [82] under a relaxed clock model and a Bayesian skyline plot demographic model. Node bars indicate the 95% HPD interval of internal nodes and sampling dates of the ancient genomes (HPD intervals of the sampling dates in parentheses). The genomes from this study are marked in red and previously published ancient genome 133 in pink. Horizontal scale denotes time in years BCE/CE.

See also Figures S5 and S6.

0 and 37 were compared, allowing duplicated regions to be covered or omitted, respectively. The annotated Nichols genome (GenBank: CP004010.2) [75] was used as reference. The observed coverage per gene of six modern TPA lineages (SS14, Mexico A, SW6, NIC2, Sea81-4, and Chicago) [41, 70, 77] was compared with the four ancient treponemal genomes from Europe (this study) and three previously published treponemal genomes from colonial Mexico [52]. Despite the reduced coverage for highly similar sequences, such as *tprC* and *tprD* genes, with mapping threshold greater than zero, a strong indication for the presence of all virulence factors in the ancient European genomes was observed. Indeed, at least a small amount of reads could be mapped specifically for all putative virulence genes, except for the *tprF* on two genomes (SJ219 and KM14-7). This absence is likely due to the low coverage of these genomes, as well as the high similarity of *tprF* gene with its paralogs (Table S3). Conversely, in the high-coverage PD28 genome, all investigated virulence factors were detected, including the *tpr* genes (Table S3). Notably, the ancient European genomes all contain the FadL family homolog TPANIC_0856, which is missing in the colonial Mexican TPA genomes 94A and 94B [52].

DISCUSSION

Early Emergence of Syphilis in Europe

In this study, four ancient *Treponema* genomes were retrieved from human skeletal remains dating to early modern Europe, providing unprecedented insights into the first reported epidemics of syphilis at the end of the 15th century. Two genomes, PD28 and SJ219, were identified as strains of syphilis-causing TPA, representing the first molecularly identified specimen of this *T. pallidum* subspecies from early modern Europe. In most of the tested settings, these genomes fall within the modern variety of the TPA strains, albeit with bootstrap values ~60–85. They form a sister clade to the modern TPA branch, basal to all its lineages with good support, when hypervariable and recombining regions are excluded. The molecular clock dating analysis of the genomes also lends support to the basal placement of these two ancient genomes with respect to the modern TPA diversity. The PD28 sample was dated to the early modern period by combined analyses of archaeological context and ^{14}C dating. Two independent radiocarbon analyses were performed on the sample SJ219 from Estonia, placing it in the early to mid-15th century, distinctly before Columbus' expeditions. This dating would place the first TPA contagions in Europe prior to the New World contact, suggesting that the original causative agent of the continent-wide epidemic at the end of the 15th century may have resided within the Old World. A reservoir effect could have influenced the radiocarbon analysis results of the individual SJ219 through the diet, and the dating could not be confirmed with certainty (STAR Methods; Figure S1). However, such direct evidence of TPA from an early European context gives unprecedented support for the existence of venereal syphilis around and potentially prior to the contact Columbus initiated in the Americas.

Table 3. Posterior Estimates of the Sampling Dates of Ancient Genomes and the Divergence Dates of Clades Inferred by Molecular Clock Dating

		Posterior Date Estimate		Posterior Probability	
Sample/Clade	Radiocarbon Date Range	Median	95% HPD Interval	Pre-Columbian	Monophyletic
133 (TPE)	1600–1861	1663.72	1600–1780.22	0	–
PD28 (TPA)	1666–1789	1713.01	1666.07–1777.66	0	–
SJ219 (TPA)	1434–1635	1535.41	1440.72–1632.46	0.278	–
CHS119 (TPE)	1450–1630	1609.09	1547.07–1629.99	0.005	–
SS14-w	–	1954.58	1927.80–1973.75	–	0.9779
SS14	–	1834.92	1729.45–1912.34	–	0.981
Nichols	–	1625.48	1485.25-1757.74	–	0.971
TPA	–	1339.12	1117.16–1515.99	–	0.977
TPE	–	1488.78	1376.73–1570.28	–	0.969
TPE/TEN	–	472.19246	–371.68–1110.10	–	0.963

Date ranges defined by radiocarbon dating were used as prior distributions for ancient sequences in the molecular clock dating analyses. The posterior probability that a sample is pre-Columbian is calculated as the proportion of posterior samples with a date <1493, and the posterior probability that a clade is monophyletic is calculated as the proportion of posterior trees where the clade is monophyletic.

Yaws-like Strains in Europe

Out of our four ancient genomes, two fell outside the variation of TPA. One of them, CHS119 from Finland, clusters with the TPE subspecies, the causative agent of yaws: an endemic treponematosis mostly restricted to tropical regions today. A direct radiocarbon dating places the sample in the 15th to 16th century, yet full confidence of the date cannot be gained due to the potential marine reservoir effect [57, 58]. Some cases of endemic treponematoses are assigned to Europe prior to the apparent eradication of the disease in the 20th century [89–91], and although the early infections' likeness to the modern clinical condition is not assured, this sample provides the first direct evidence of a TPE infection in historical Northern Europe, far from its typical present-day distribution. Strikingly, the contemporaneous genome KM14-7 from the Netherlands falls basal to both the bejel- and yaws-causing lineages, unveiling a previously unidentified lineage of *T. pallidum*.

The low sequencing coverage obtained for the KM14-7 genome prevented its inclusion in the recombination and time-calibrated phylogenetic analysis. However, the ML tree topology with KM14-7 in the basal position to TPE and TEN clades was further confirmed through closer inspection at the nucleotide level. The lineage shows genetic similarities to both current TPA (12 characteristic SNPs) and TPE/TEN (18 characteristic SNPs) strains but represents a distinct form from both and has apparently diverged from their common ancestor before TPE and TEN divergence, which we dated to at least 1,000 years BP. Altogether, our ancient treponemal genomes from northern and central Europe point to an early-existing diversity of *T. pallidum* in the Old World. Their existence does not refute the potential introduction of new strains of treponemes from the New World in the wake of the European expeditions yet lends credibility to a potentially endemic origin of the 15th century epidemics.

Whereas recombination events between the three modern-day treponemal subspecies are deemed rare [92], such events were observed across the subspecies in our study. These recombination events presumably happened in the past, before TPA, TPE, and TEN acquired their currently separated geographical niches [41, 52]. Contemporaneous historical cases of syphilis and yaws in a geographically overlapping region provide a plausible opportunity for recombination [73, 76]. The potential recombination events observed in this study involved lineages from the modern-day diversity, the ancient genomes PD28 and CHS119 from Europe, and 94A and 94B genomes from Mexico [52].

Overall, our observations point to recombination events that are directed toward the syphilis-causing clades from the yaws- and bejel-causing ancestors. The recombinations between the clades further support a geographically close common history of the TPA and TPE lineages, which cannot be concluded from the geographical distribution of extant lineages.

Old Hypotheses Revisited

Assuming the ancient infectious agents had similar clinical manifestations to modern-day *T. pallidum* subspecies, the reconstructed TPA and TPE genomes from ancient Finnish and Estonian human remains are showing an early spread of both venereal syphilis and yaws at the northern end of Europe. Although the ^{14}C analyses and the archaeological context of the individuals CHS119 and SJ219 support pre-Columbian dating, these claims are thwarted by methodological uncertainties (STAR Methods; Figure S1). In addition to the direct dating of the individual samples, we used our novel ancient genomes for molecular dating of the phylogenetic clades of *T. pallidum* (Figure 3). This dating analysis sets the T_{MRCA} for the entire *T. pallidum* family to at least 1000 BCE. The available calibration points, however, provide only the lower bound for the subspecies' divergence, permitting a possibility of a deep prehistoric background of treponemes in association with their human hosts [25, 26]. The T_{MRCA} for all TPA strains between the 10th and 15th centuries CE supports a radiation of these strains within Europe instead of having a single ancestral source from the New World. The separation of TPE and TEN clades between 9th century BCE and 10th century CE clearly predates contact period and, together with the genome KM14-7 and its

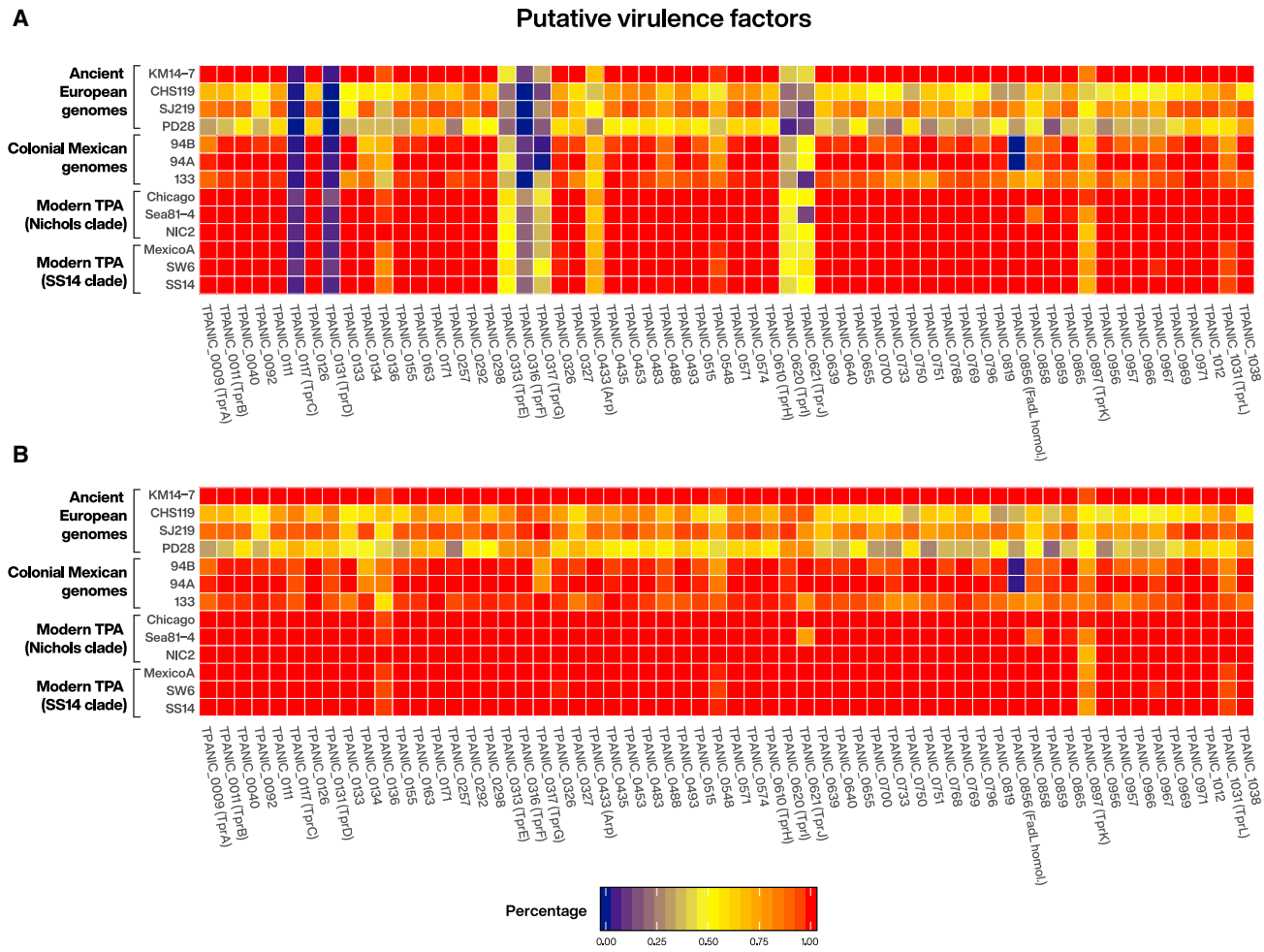

Figure 4. Virulence Analysis

A heatmap visualization of 60 putative virulence genes analyzed on the four ancient genomes from early modern Europe (Ancient European genomes) based on Nichols reference genome (CP004010.2) annotation, in comparison with a selection of six modern TPA strains, three from Nichols and SS14 clades each, and the previously published colonial Mexican genomes [52], using (A) a quality filtering threshold of 37, excluding any mapping of reads, should the exact region appear more than once along the genome and (B) a quality filtering threshold of 0, i.e., allowing a mapping of reads on identical regions. See also Table S3.

ancestral characteristics, suggests a common history of these diseases in the Old World. All currently known lineages of yaws have a common ancestor as late as 14th to 16th century CE, which could point to a novel radiation simultaneously with the rise of the early venereal syphilis, possibly enabled by the same evolutionary opportunities around the contact period or due to competition between concurrent subspecies.

The KM14-7 genome represents a possibly unprecedented type of treponemal infectious agent that possessed genetic similarities to both currently existing syphilis and yaws yet appears to have been distinct from both. In its pathogenesis, this agent may have resembled endemic treponematoses, because the majority of its recovered SNPs are shared with the yaws and bejel lineages. It has been suggested that yaws or its ancestors represent the original form of treponematosis that appeared and spread around the world thousands of years ago, was then re-introduced to the Iberian Peninsula via the Central and Western African slave trade some 50 years before Columbus' travels, and eventually gave rise to the venereal syphilis [42, 93]. It is indeed possible that the venereal form in the Old World developed from an endemic type of disease, enhanced by genetic recombination events or in response to a competition between existing pathogens [34, 38]. Likewise, recombination events may have occurred between the endemic European strains and novel lineages introduced in the wake of the New World contact, precipitating the epidemic events at that time. Although cladality between the different subspecies clearly exists in both the past and present, it now seems likely that recombination has interconnected these clades in the past and that the genetic differences do not necessarily define the treponemal pathogenesis observed in the archaeological remains. Furthermore, recent studies of apparently endemic cases of sexually transmitted bejel from Japan and Cuba possess potential to challenge the modern-day views on geographical and etiological particularity and transmission routes of the different subspecies [9, 94]. Recombination occurring between TPA and TEN clades

has been proposed as a plausible course of evolution, leading to these still poorly known local strains, the Bosnia A bejel-causing strain, and an isolate 11q/j found from a syphilis-like lesion in a bejel patient [76, 95]. These recombination events may stem from a historical time that provided more geographical overlap and thus allowed encounters between *T. pallidum* subspecies.

Our data show that all genes associated with virulence in modern *T. pallidum* strains were likely already present in ancient European strains. In particular, the *FadL* homolog gene, possibly representing a deletion specific to the colonial Mexican strains, was recovered in all the ancient European genomes reported here. Thus, any excess of virulence potentially developed by *T. pallidum* during the second half of the 20th century was likely not through novel gene acquisition. To ascertain the alleged gradual reduction of virulence in syphilis after the initial European outbreak and highlight possible changes in protein functions coded by individual genes, more detailed sequence comparisons between ancient and modern genomes would be required, likely accompanied by *de novo* approaches with functional predictions that are beyond assessing with our current low-coverage data. Apart from the etiology and sequence diversity of these newly discovered ancient genomes, many past *T. pallidum* lineages can be presumed to remain entirely unknown today. Once revealed, they may prove pivotal in uncovering the relationship between treponemal strains and dating their emergence.

Outlook and Implications on Sampling Strategies

Retrieving treponemal DNA from skeletal material is highly challenging, and the feasibility of the effort was widely questioned before the recently published colonial Mexican genomes [49, 50, 52]. Furthermore, diagnostic signs between endemic and venereal syphilis are difficult to distinguish, especially in skeletal remains, and several forms of treponematoses appear to have existed concurrently in early modern Europe. Although the previously published Mexican genomes were obtained only from neonates and infants [52], our four positive cases represent both non-adult (KM14-7, SJ219, and PD28) and adult (CHS119) individuals, including one only tentatively diagnosed case of treponematosis (SJ219). Successful retrieval of treponemal DNA was likely facilitated by sampling hard tissue directly involved with an ongoing inflammatory response, such as an active lesion (KM14-7), or one possessing ample blood flow, such as dental cavity (CHS119). With the perinatal sample (PD28), we witnessed the first retrieval of pathogen DNA from a petrous bone, yielding an ancient TPA genome with up to 136-fold coverage. Presumably, an extremely high bacterial load that contributed to this exceptionally successful case was a consequence of an early, systemic congenital infection [96]. Retrieving ancient treponemal DNA from such a large variety of skeletal materials raises hopes of achieving future progress with the paleopathological cases of advanced and latent infections. Altogether, we were able to reconstruct four ancient treponemal genomes, from two of the known subspecies and one formerly unknown strain. These cases support the notion that different treponemal agents cause essentially similar skeletal alterations and are highly adaptable to environmental circumstances [40, 97]. We therefore propose that the geographical separation criteria between treponemal diseases should be used with caution, especially when related to earlier forms of treponematoses and their diagnostic manifestations within the archaeological record. Improving methodologies specifically targeted for samples with low bacterial load or sparse genomic coverage may soon aid in recovering positive ancient DNA results from putative cases of treponematoses from early- to prehistoric contexts, thereby illuminating the most persistent quandaries of the field, including the ultimate origin of venereal syphilis.

STAR★METHODS

Detailed methods are provided in the online version of this paper and include the following:

- KEY RESOURCES TABLE
- RESOURCE AVAILABILITY
  - Lead Contact
  - Materials Availability
  - Data and Code Availability
- EXPERIMENTAL MODEL AND SUBJECT DETAILS
  - Ethical approvals
  - Description of archaeological contexts and sample selection
- METHOD DETAILS
  - Sample processing
  - Reservoir effect correction of the CHS119 sample
  - Sampling and DNA extraction
  - Library preparation
  - Double-stranded DNA library preparation
  - Uracil-DNA Glycosylase (UDG) treated double-stranded DNA library preparation
  - Single-stranded DNA library preparation
  - Capture techniques
  - Sequencing
  - Read processing, mapping and variant calling
  - Genomic dataset and multisequence alignment
  - SNP quality assessment
  - Phylogenetic and recombination analysis
  - KM14-7 SNP analysis
  - Molecular clock dating
  - Robustness of molecular clock dating
  - Virulence analysis
- QUANTIFICATION AND STATISTICAL ANALYSIS
  - *In silico* screening
  - Phylogenetic analysis
  - Molecular clock test
  - Dating analysis

SUPPLEMENTAL INFORMATION

Supplemental Information can be found online at https://doi.org/10.1016/j.cub.2020.07.058.

ACKNOWLEDGMENTS

We would like to thank Abagail Breidenstein for proofreading of the manuscript; Benito Casagrande, Sirkku Pihlman, Liisa Seppänen, and the working committee of the Holy Ghost Chapel for permission to sample and curation of the Turku skeletal material; Marianna Niukkanen, Jutta Kuitunen, The

Finnish Heritage Agency, and Porvoo Church for permission to sample and curation of the Porvoo skeletal material; and Gemeente Zwolle for permission to sample the Kampen skeletal material. Figure graphics and layouts were designed by Michelle O'Reilly at the Max Planck Institute for the Science of Human History, Jena. This work was supported by the Swiss National Science Foundation: grant number 188963—"Towards the origins of syphilis" (V.J.S. and K.M.), the University of Zurich's University Research Priority Program "Evolution in Action: From Genomes to Ecosystems" (V.J.S. and J.N.), the Max Planck Society (J.K.), the Senckenberg Centre for Human Evolution and Palaeoenvironment (S-HEP) at the University of Tübingen (V.J.S. and J.K.), the Emil Aaltonen Foundation (K.M.), the Kone Foundation (K.M., P.O., and K.S.) and Aatos Erkko Foundation (K.M., P.O., and K.S.), Otto A. Malm Foundation (K.S.) and University of Helsinki Research Foundation (K.S.), the European Research Council under the Seventh Framework Programme (FP7/2007-2013)—grant agreement 614725—PATHPHYLODYN (L.d.-P.), the Oxford Martin School (L.d.-P.), University of Tartu's Institute of Genomics project "Natural selection and migrations in shaping human genetic diversity in East European Plain. An ancient DNA study" (PRG243; H.V., A. Kriiska, and M.M.), and grants BFU2017-89594R (M.P.-D. and F.G.-C.) and FPU2017-02367 (M.P.-D.) from MICIN and Prometeo2016-0122 from Generalitat Valenciana (M.P.-D. and F.G.-C.).

AUTHOR CONTRIBUTIONS

V.J.S., K.M., and J.K. conceived and designed the study. K.S., R.S., S.I., M.O., H.V., M.M., and A. Kriiska provided samples and archaeological context. V.J.S., F.G.-C., D.K., and J.K. supervised the work. S.P., K.M., and G.A. performed the experimental work. K.M., J.N., A. Kocher, L.d.-P., M.P.-D., F.G.-C., and D.K. analyzed the sequenced data. K.M. and V.J.S. wrote the manuscript with input from all authors. All authors reviewed the manuscript.

DECLARATION OF INTERESTS

The authors declare no competing interests.

Received: February 19, 2020
Revised: April 24, 2020
Accepted: July 16, 2020
Published: August 13, 2020

REFERENCES

1. Kent, M.E., and Romanelli, F. (2008). Reexamining syphilis: an update on epidemiology, clinical manifestations, and management. Ann. Pharmacother. *42*, 226–236.
2. Mitjà, O., Šmajs, D., and Bassat, Q. (2013). Advances in the diagnosis of endemic treponematoses: yaws, bejel, and pinta. PLoS Negl. Trop. Dis. *7*, e2283.
3. Giacani, L., and Lukehart, S.A. (2014). The endemic treponematoses. Clin. Microbiol. Rev. *27*, 89–115.
4. Šmajs, D., Strouhal, M., and Knauf, S. (2018). Genetics of human and animal uncultivable treponemal pathogens. Infect. Genet. Evol. *61*, 92–107.
5. Kazadi, W.M., Asiedu, K.B., Agana, N., and Mitjà, O. (2014). Epidemiology of yaws: an update. Clin. Epidemiol. *6*, 119–128.
6. Spiteri, G., Unemo, M., Mårdh, O., and Amato-Gauci, A.J. (2019). The resurgence of syphilis in high-income countries in the 2000s: a focus on Europe. Epidemiol. Infect. *147*, e143.
7. Mitjà, O., Godornes, C., Houinei, W., Kapa, A., Paru, R., Abel, H., González-Beiras, C., Bieb, S.V., Wangi, J., Barry, A.E., et al. (2018). Re-emergence of yaws after single mass azithromycin treatment followed by targeted treatment: a longitudinal study. Lancet *391*, 1599–1607.
8. Beale, M.A., Marks, M., Sahi, S.K., Tantalo, L.C., Nori, A.V., French, P., Lukehart, S.A., Marra, C.M., and Thomson, N.R. (2019). Genomic epidemiology of syphilis reveals independent emergence of macrolide resistance across multiple circulating lineages. Nat. Commun. *10*, 3255.
9. Kawahata, T., Kojima, Y., Furubayashi, K., Shinohara, K., Shimizu, T., Komano, J., Mori, H., and Motomura, K. (2019). Bejel, a nonvenereal treponematosis, among men who have sex with men, Japan. Emerg. Infect. Dis. *25*, 1581–1583.
10. Stamm, L.V., Stapleton, J.T., and Bassford, P.J., Jr. (1988). In vitro assay to demonstrate high-level erythromycin resistance of a clinical isolate of Treponema pallidum. Antimicrob. Agents Chemother. *32*, 164–169.
11. Šmajs, D., Paštěková, L., and Grillová, L. (2015). Macrolide resistance in the syphilis spirochete, Treponema pallidum ssp. pallidum: can we also expect macrolide-resistant yaws strains? Am. J. Trop. Med. Hyg. *93*, 678–683.
12. Stamm, L.V. (2016). Syphilis: re-emergence of an old foe. Microb. Cell *3*, 363–370.
13. Mitjà, O., Asiedu, K., and Mabey, D. (2013). Yaws. Lancet *381*, 763–773.
14. Radolf, J.D. (1996). Treponema. In Medical Microbiology, Fourth Edition, , S. Baron, ed. (University of Texas Medical Branch at Galveston).
15. Lafond, R.E., and Lukehart, S.A. (2006). Biological basis for syphilis. Clin. Microbiol. Rev. *19*, 29–49.
16. Norris, S.J., Cox, D.L., and Weinstock, G.M. (2001). Biology of Treponema pallidum: correlation of functional activities with genome sequence data. J. Mol. Microbiol. Biotechnol. *3*, 37–62.
17. Knell, R.J. (2004). Syphilis in renaissance Europe: rapid evolution of an introduced sexually transmitted disease? Proc. Biol. Sci. *271* (*Suppl 4*), S174–S176.
18. Fenton, K.A., Breban, R., Vardavas, R., Okano, J.T., Martin, T., Aral, S., and Blower, S. (2008). Infectious syphilis in high-income settings in the 21st century. Lancet Infect. Dis. *8*, 244–253.
19. Giacani, L., Molini, B.J., Kim, E.Y., Godornes, B.C., Leader, B.T., Tantalo, L.C., Centurion-Lara, A., and Lukehart, S.A. (2010). Antigenic variation in Treponema pallidum: TprK sequence diversity accumulates in response to immune pressure during experimental syphilis. J. Immunol. *184*, 3822–3829.
20. Tampa, M., Sarbu, I., Matei, C., Benea, V., and Georgescu, S.R. (2014). Brief history of syphilis. J. Med. Life *7*, 4–10.
21. Tognotti, E. (2009). The rise and fall of syphilis in Renaissance Europe. J. Med. Humanit. *30*, 99–113.
22. Arrizabalaga, J. (1993). Syphilis. In The Cambridge World History of Human Disease, K.F. Kiple, ed. (Cambridge University), pp. 1025–1033.
23. Harper, K.N., Zuckerman, M.K., Harper, M.L., Kingston, J.D., and Armelagos, G.J. (2011). The origin and antiquity of syphilis revisited: an appraisal of Old World pre-Columbian evidence for treponemal infection. Am. J. Phys. Anthropol. *146* (*Suppl 53*), 99–133.
24. Rothschild, B.M. (2005). History of syphilis. Clin. Infect. Dis. *40*, 1454–1463.
25. Hackett, C.J. (1963). On the origin of the human treponematoses (pinta, yaws, endemic syphilis and venereal syphilis). Bull. World Health Organ. *29*, 7–41.
26. Cockburn, T.A. (1961). The origin of the treponematoses. Bull. World Health Organ. *24*, 221–228.
27. Meyer, C., Jung, C., Kohl, T., Poenicke, A., Poppe, A., and Alt, K.W. (2002). Syphilis 2001–a palaeopathological reappraisal. Homo *53*, 39–58.
28. Crane-Kramer, G.M. (2000). The paleoepidemiological examination of treponemal infection and leprosy in medieval populations from northern Europe. PhD thesis (University of Calgary).
29. Henneberg, M., and Henneberg, R.J. (1994). Treponematosis in an ancient Greek colony of Metaponto, southern Italy, 580–250 BCE. The Origin of Syphilis in Europe: Before or After *1493*, 92–98.
30. Blondiaux, J., and Bagousse, A.A. (1994). A treponematosis dated from the Late Roman Empire in Normandie, France. L'Origine de la Syphilis en Europe: Avant ou Aprés *1493*, 99–100.

31. Fonseca, E., García-Silva, J., del Pozo, J., Yebra, M.T., Cuevas, J., and Contreras, F. (1999). Syphilis in an HIV infected patient misdiagnosed as leprosy. J. Cutan. Pathol. *26*, 51–54.

32. Bruisten, S.M. (2012). Protocols for detection and typing of Treponema pallidum using PCR methods. Methods Mol. Biol. *903*, 141–167.

33. Grillová, L., Bawa, T., Mikalová, L., Gayet-Ageron, A., Nieselt, K., Strouhal, M., Sednaoui, P., Ferry, T., Cavassini, M., Lautenschlager, S., et al. (2018). Molecular characterization of Treponema pallidum subsp. pallidum in Switzerland and France with a new multilocus sequence typing scheme. PLoS ONE *13*, e0200773.

34. Hudson, E.H. (1965). Treponematosis and man's social evolution. Am. Anthropol. *67*, 885–901.

35. Powell, M.L., and Cook, D.C. (2005). The Myth of Syphilis: The Natural History of Treponematosis in North America (University Press of Florida).

36. Centurion-Lara, A., Molini, B.J., Godornes, C., Sun, E., Hevner, K., Van Voorhis, W.C., and Lukehart, S.A. (2006). Molecular differentiation of Treponema pallidum subspecies. J. Clin. Microbiol. *44*, 3377–3380.

37. Mikalová, L., Strouhal, M., Čejková, D., Zobaníková, M., Pospíšilová, P., Norris, S.J., Sodergren, E., Weinstock, G.M., and Šmajs, D. (2010). Genome analysis of Treponema pallidum subsp. pallidum and subsp. pertenue strains: most of the genetic differences are localized in six regions. PLoS ONE *5*, e15713.

38. Gray, R.R., Mulligan, C.J., Molini, B.J., Sun, E.S., Giacani, L., Godornes, C., Kitchen, A., Lukehart, S.A., and Centurion-Lara, A. (2006). Molecular evolution of the tprC, D, I, K, G, and J genes in the pathogenic genus Treponema. Mol. Biol. Evol. *23*, 2220–2233.

39. Ho, E.L., and Lukehart, S.A. (2011). Syphilis: using modern approaches to understand an old disease. J. Clin. Invest. *121*, 4584–4592.

40. Mulligan, C.J., Norris, S.J., and Lukehart, S.A. (2008). Molecular studies in Treponema pallidum evolution: toward clarity? PLoS Negl. Trop. Dis. *2*, e184.

41. Arora, N., Schuenemann, V.J., Jäger, G., Peltzer, A., Seitz, A., Herbig, A., Strouhal, M., Grillová, L., Sánchez-Busó, L., Kühnert, D., et al. (2016). Origin of modern syphilis and emergence of a pandemic Treponema pallidum cluster. Nat. Microbiol. *2*, 16245.

42. de Melo, F.L., de Mello, J.C.M., Fraga, A.M., Nunes, K., and Eggers, S. (2010). Syphilis at the crossroad of phylogenetics and paleopathology. PLoS Negl. Trop. Dis. *4*, e575.

43. Cui, Y., Yu, C., Yan, Y., Li, D., Li, Y., Jombart, T., Weinert, L.A., Wang, Z., Guo, Z., Xu, L., et al. (2013). Historical variations in mutation rate in an epidemic pathogen, Yersinia pestis. Proc. Natl. Acad. Sci. USA *110*, 577–582.

44. Spyrou, M.A., Bos, K.I., Herbig, A., and Krause, J. (2019). Ancient pathogen genomics as an emerging tool for infectious disease research. Nat. Rev. Genet. *20*, 323–340.

45. Bos, K.I., Schuenemann, V.J., Golding, G.B., Burbano, H.A., Waglechner, N., Coombes, B.K., McPhee, J.B., DeWitte, S.N., Meyer, M., Schmedes, S., et al. (2011). A draft genome of Yersinia pestis from victims of the Black Death. Nature *478*, 506–510.

46. Schuenemann, V.J., Singh, P., Mendum, T.A., Krause-Kyora, B., Jäger, G., Bos, K.I., Herbig, A., Economou, C., Benjak, A., Busso, P., et al. (2013). Genome-wide comparison of medieval and modern Mycobacterium leprae. Science *341*, 179–183.

47. Bos, K.I., Harkins, K.M., Herbig, A., Coscolla, M., Weber, N., Comas, I., Forrest, S.A., Bryant, J.M., Harris, S.R., Schuenemann, V.J., et al. (2014). Pre-Columbian mycobacterial genomes reveal seals as a source of New World human tuberculosis. Nature *514*, 494–497.

48. Fraser, C.M., Norris, S.J., Weinstock, G.M., White, O., Sutton, G.G., Dodson, R., Gwinn, M., Hickey, E.K., Clayton, R., Ketchum, K.A., et al. (1998). Complete genome sequence of Treponema pallidum, the syphilis spirochete. Science *281*, 375–388.

49. Bouwman, A.S., and Brown, T.A. (2005). The limits of biomolecular palaeopathology: ancient DNA cannot be used to study venereal syphilis. J. Archaeol. Sci. *32*, 703–713.

50. von Hunnius, T.E., Yang, D., Eng, B., Waye, J.S., and Saunders, S.R. (2007). Digging deeper into the limits of ancient DNA research on syphilis. J. Archaeol. Sci. *34*, 2091–2100.

51. Montiel, R., Solórzano, E., Díaz, N., Álvarez-Sandoval, B.A., González-Ruiz, M., Cañadas, M.P., Simões, N., Isidro, A., and Malgosa, A. (2012). Neonate human remains: a window of opportunity to the molecular study of ancient syphilis. PLoS ONE *7*, e36371.

52. Schuenemann, V.J., Kumar Lankapalli, A., Barquera, R., Nelson, E.A., Iraíz Hernández, D., Acuña Alonzo, V., Bos, K.I., Márquez Morfín, L., Herbig, A., and Krause, J. (2018). Historic Treponema pallidum genomes from colonial Mexico retrieved from archaeological remains. PLoS Negl. Trop. Dis. *12*, e0006447.

53. Hofreiter, M., Paijmans, J.L.A., Goodchild, H., Speller, C.F., Barlow, A., Fortes, G.G., Thomas, J.A., Ludwig, A., and Collins, M.J. (2015). The future of ancient DNA: technical advances and conceptual shifts. BioEssays *37*, 284–293.

54. Mitchell, P.D., and Brickley, M. (2017). Updated Guidelines to the Standards for Recording Human Remains (Institute of Field Archaeologists).

55. Salo, K. (2007). Osteologinen Analyysi. Porvoo, Porvoon Kirkko 2007 (Archives of the National Board of Antiquities in Finland).

56. Crabtree, J., Agrawal, S., Mahurkar, A., Myers, G.S., Rasko, D.A., and White, O. (2014). Circleator: flexible circular visualization of genome-associated data with BioPerl and SVG. Bioinformatics *30*, 3125–3127.

57. Etu-Sihvola, H., Bocherens, H., Drucker, D.G., Junno, A., Mannermaa, K., Oinonen, M., Uusitalo, J., and Arppe, L. (2019). The dIANA database–resource for isotopic paleodietary research in the Baltic Sea area. J. Archaeol. Sci. Rep. *24*, 1003–1013.

58. Oinonen, M., Alenius, T., Arppe, L., Bocherens, H., Etu-Sihvola, H., Helama, S., Huhtamaa, H., Lahtinen, M., Mannermaa, K., Onkamo, P., et al. (2020). Buried in water, burdened by nature-Resilience carried the Iron Age people through Fimbulvinter. PLoS ONE *15*, e0231787.

59. Hodges, E., Rooks, M., Xuan, Z., Bhattacharjee, A., Benjamin Gordon, D., Brizuela, L., Richard McCombie, W., and Hannon, G.J. (2009). Hybrid selection of discrete genomic intervals on custom-designed microarrays for massively parallel sequencing. Nat. Protoc. *4*, 960–974.

60. Briggs, A.W., Stenzel, U., Johnson, P.L.F., Green, R.E., Kelso, J., Prüfer, K., Meyer, M., Krause, J., Ronan, M.T., Lachmann, M., and Pääbo, S. (2007). Patterns of damage in genomic DNA sequences from a Neandertal. Proc. Natl. Acad. Sci. USA *104*, 14616–14621.

61. Sawyer, S., Krause, J., Guschanski, K., Savolainen, V., and Pääbo, S. (2012). Temporal patterns of nucleotide misincorporations and DNA fragmentation in ancient DNA. PLoS ONE *7*, e34131.

62. Briggs, A.W., Stenzel, U., Meyer, M., Krause, J., Kircher, M., and Pääbo, S. (2010). Removal of deaminated cytosines and detection of in vivo methylation in ancient DNA. Nucleic Acids Res. *38*, e87.

63. Maricic, T., Whitten, M., and Pääbo, S. (2010). Multiplexed DNA sequence capture of mitochondrial genomes using PCR products. PLoS ONE *5*, e14004.

64. Weissensteiner, H., Pacher, D., Kloss-Brandstätter, A., Forer, L., Specht, G., Bandelt, H.-J., Kronenberg, F., Salas, A., and Schönherr, S. (2016). HaploGrep 2: mitochondrial haplogroup classification in the era of high-throughput sequencing. Nucleic Acids Res. *44* (W1), W58–W63.

65. van Oven, M., and Kayser, M. (2009). Updated comprehensive phylogenetic tree of global human mitochondrial DNA variation. Hum. Mutat. *30*, E386–E394.

66. Renaud, G., Slon, V., Duggan, A.T., and Kelso, J. (2015). Schmutzi: estimation of contamination and endogenous mitochondrial consensus calling for ancient DNA. Genome Biol. *16*, 224.

67. Mittnik, A., Wang, C.-C., Svoboda, J., and Krause, J. (2016). A molecular approach to the sexing of the triple burial at the upper Paleolithic site of Dolní Věstonice. PLoS ONE *11*, e0163019.

68. Skoglund, P., Storå, J., Götherström, A., and Jakobsson, M. (2013). Accurate sex identification of ancient human remains using DNA shotgun sequencing. J. Archaeol. Sci. *40*, 4477–4482.

69. Peltzer, A., Jäger, G., Herbig, A., Seitz, A., Kniep, C., Krause, J., and Nieselt, K. (2016). EAGER: efficient ancient genome reconstruction. Genome Biol. *17*, 60.

70. Giacani, L., Jeffrey, B.M., Molini, B.J., Le, H.T., Lukehart, S.A., Centurion-Lara, A., and Rockey, D.D. (2010). Complete genome sequence and annotation of the Treponema pallidum subsp. pallidum Chicago strain. J. Bacteriol. *192*, 2645–2646.

71. Zobaníková, M., Mikolka, P., Cejková, D., Pospíšilová, P., Chen, L., Strouhal, M., Qin, X., Weinstock, G.M., and Smajs, D. (2012). Complete genome sequence of Treponema pallidum strain DAL-1. Stand. Genomic Sci. *7*, 12–21.

72. Cejková, D., Zobaníková, M., Chen, L., Pospíšilová, P., Strouhal, M., Qin, X., Mikalová, L., Norris, S.J., Muzny, D.M., Gibbs, R.A., et al. (2012). Whole genome sequences of three Treponema pallidum ssp. pertenue strains: yaws and syphilis treponemes differ in less than 0.2% of the genome sequence. PLoS Negl. Trop. Dis. *6*, e1471.

73. Pětrošová, H., Zobaníková, M., Čejková, D., Mikalová, L., Pospíšilová, P., Strouhal, M., Chen, L., Qin, X., Muzny, D.M., Weinstock, G.M., and Šmajs, D. (2012). Whole genome sequence of Treponema pallidum ssp. pallidum, strain Mexico A, suggests recombination between yaws and syphilis strains. PLoS Negl. Trop. Dis. *6*, e1832.

74. Zobaníková, M., Strouhal, M., Mikalová, L., Cejková, D., Ambrožová, L., Pospíšilová, P., Fulton, L.L., Chen, L., Sodergren, E., Weinstock, G.M., and Smajs, D. (2013). Whole genome sequence of the Treponema Fribourg-Blanc: unspecified simian isolate is highly similar to the yaws subspecies. PLoS Negl. Trop. Dis. *7*, e2172.

75. Pětrošová, H., Pospíšilová, P., Strouhal, M., Čejková, D., Zobaníková, M., Mikalová, L., Sodergren, E., Weinstock, G.M., and Šmajs, D. (2013). Resequencing of Treponema pallidum ssp. pallidum strains Nichols and SS14: correction of sequencing errors resulted in increased separation of syphilis treponeme subclusters. PLoS ONE *8*, e74319.

76. Staudová, B., Strouhal, M., Zobaníková, M., Cejková, D., Fulton, L.L., Chen, L., Giacani, L., Centurion-Lara, A., Bruisten, S.M., Sodergren, E., et al. (2014). Whole genome sequence of the Treponema pallidum subsp. endemicum strain Bosnia A: the genome is related to yaws treponemes but contains few loci similar to syphilis treponemes. PLoS Negl. Trop. Dis. *8*, e3261.

77. Giacani, L., Iverson-Cabral, S.L., King, J.C.K., Molini, B.J., Lukehart, S.A., and Centurion-Lara, A. (2014). Complete Genome Sequence of the Treponema pallidum subsp. pallidum Sea81-4 Strain. Genome Announc. *2*, e00333-14.

78. Sun, J., Meng, Z., Wu, K., Liu, B., Zhang, S., Liu, Y., Wang, Y., Zheng, H., Huang, J., and Zhou, P. (2016). Tracing the origin of *Treponema pallidum* in China using next-generation sequencing. Oncotarget *7*, 42904–42918.

79. Paradis, E., and Schliep, K. (2019). ape 5.0: an environment for modern phylogenetics and evolutionary analyses in R. Bioinformatics *35*, 526–528.

80. Galili, T. (2015). dendextend: an R package for visualizing, adjusting and comparing trees of hierarchical clustering. Bioinformatics *31*, 3718–3720.

81. Duchêne, S., Duchêne, D., Holmes, E.C., and Ho, S.Y.W. (2015). The performance of the date-randomization test in phylogenetic analyses of time-structured virus data. Mol. Biol. Evol. *32*, 1895–1906.

82. Bouckaert, R., Vaughan, T.G., Barido-Sottani, J., Duchêne, S., Fourment, M., Gavryushkina, A., Heled, J., Jones, G., Kühnert, D., De Maio, N., et al. (2019). BEAST 2.5: an advanced software platform for Bayesian evolutionary analysis. PLoS Comput. Biol. *15*, e1006650.

83. Navascués, M., and Emerson, B.C. (2009). Elevated substitution rate estimates from ancient DNA: model violation and bias of Bayesian methods. Mol. Ecol. *18*, 4390–4397.

84. Meyer, A.G., Spielman, S.J., Bedford, T., and Wilke, C.O. (2015). Time dependence of evolutionary metrics during the 2009 pandemic influenza virus outbreak. Virus Evol. *1*, vev006.

85. Ho, S.Y.W., Duchêne, S., Molak, M., and Shapiro, B. (2015). Time-dependent estimates of molecular evolutionary rates: evidence and causes. Mol. Ecol. *24*, 6007–6012.

86. Düx, A., Lequime, S., Patrono, L.V., Vrancken, B., Boral, S., Gogarten, J.F., Hilbig, A., Horst, D., Merkel, K., Prepoint, B., et al. (2020). Measles virus and rinderpest virus divergence dated to the sixth century BCE. Science *368*, 1367–1370.

87. Weinstock, G.M., Hardham, J.M., McLeod, M.P., Sodergren, E.J., and Norris, S.J. (1998). The genome of Treponema pallidum: new light on the agent of syphilis. FEMS Microbiol. Rev. *22*, 323–332.

88. Radolf, J.D., Deka, R.K., Anand, A., Šmajs, D., Norgard, M.V., and Yang, X.F. (2016). Treponema pallidum, the syphilis spirochete: making a living as a stealth pathogen. Nat. Rev. Microbiol. *14*, 744–759.

89. Morton, R.S. (1964). The button scurvy of Ireland: postscript of the MSSVD meeting in Dublin, May 29 and 30, 1964. Br. J. Vener. Dis. *40*, 271–272.

90. Morton, R.S. (1967). The sibbens of Scotland. Med. Hist. *11*, 374–380.

91. Morton, R.S. (1968). Another look at the Morbus Gallicus. Postscript to the meeting of the Medical Society for the Study of Venereal Diseases, Geneva, May 26-28, 1967. Br. J. Vener. Dis. *44*, 174–177.

92. Achtman, M. (2008). Evolution, population structure, and phylogeography of genetically monomorphic bacterial pathogens. Annu. Rev. Microbiol. *62*, 53–70.

93. Hoeppli, R. (1969). Parasitic diseases in Africa and the Western Hemisphere. Early documentation and transmission by the slave trade. Acta Trop. Suppl. *10*, 1–240.

94. Noda, A.A., Grillová, L., Lienhard, R., Blanco, O., Rodríguez, I., and Šmajs, D. (2018). Bejel in Cuba: molecular identification of Treponema pallidum subsp. endemicum in patients diagnosed with venereal syphilis. Clin. Microbiol. Infect. *24*, 1210.e1–1210.e5.

95. Mikalová, L., Strouhal, M., Oppelt, J., Grange, P.A., Janier, M., Benhaddou, N., Dupin, N., and Šmajs, D. (2017). Human Treponema pallidum 11q/j isolate belongs to subsp. endemicum but contains two loci with a sequence in TP0548 and TP0488 similar to subsp. pertenue and subsp. pallidum, respectively. PLoS Negl. Trop. Dis. *11*, e0005434.

96. Ilagan, N.B., Weyhing, B., Liang, K.C., Womack, S.J., and Shankaran, S. (1993). Congenital syphilitic skeletal manifestations in a premature infant revisited. Clin. Pediatr. (Phila.) *32*, 312–313.

97. Antal, G.M., Lukehart, S.A., and Meheus, A.Z. (2002). The endemic treponematoses. Microbes Infect. *4*, 83–94.

98. Meyer, M., and Kircher, M. (2010). Illumina sequencing library preparation for highly multiplexed target capture and sequencing. Cold Spring Harb. Protoc. *2010*, pdb.prot5448.

99. Broad Institute (2019). Picard tools. http://broadinstitute.github.io/picard/.

100. Jónsson, H., Ginolhac, A., Schubert, M., Johnson, P.L.F., and Orlando, L. (2013). mapDamage2.0: fast approximate Bayesian estimates of ancient DNA damage parameters. Bioinformatics *29*, 1682–1684.

101. Van der Auwera, G.A., Carneiro, M.O., Hartl, C, Poplin, R., Del Angel, G., Levy-Moonshine, A., Jordan, T., Shakir, K., Roazen, D., Thibault, J., et al. (2013). From FastQ data to high confidence variant calls: the Genome Analysis Toolkit best practices pipeline. Curr. Protoc. Bioinformatics *43*, 11.10.1–11.10.33.

102. Herbig, A. (2020). MultiVCFAnalyzer. https://github.com/alexherbig/MultiVCFAnalyzer.

103. Quinlan, A.R., and Hall, I.M. (2010). BEDTools: a flexible suite of utilities for comparing genomic features. Bioinformatics *26*, 841–842.

104. Wickham, H. (2009). ggplot2: Elegant Graphics for Data Analysis (Springer).

105. Wickham, H. (2016). ggplot2: Elegant Graphics for Data Analysis (Springer).

106. R Studio Team (2015). RStudio: integrated development for R (RStudio).

107. Kroepelin, A. (2020). SNP_Evaluation (Github). https://github.com/andreasKroepelin/SNP_Evaluation.

108. Keller, M., Spyrou, M.A., Scheib, C.L., Neumann, G.U., Kröpelin, A., Haas-Gebhard, B., Päffgen, B., Haberstroh, J., Ribera i Lacomba, A., Raynaud, C., et al. (2019). Ancient Yersinia pestis genomes from across Western Europe reveal early diversification during the First Pandemic (541–750). Proc. Natl. Acad. Sci. USA *116*, 12363–12372.

109. Andrews, S. (2010). FastQC: a quality control tool for high throughput sequence data. https://www.bioinformatics.babraham.ac.uk/projects/fastqc/.

110. Nguyen, L.-T., Schmidt, H.A., von Haeseler, A., and Minh, B.Q. (2015). IQ-TREE: a fast and effective stochastic algorithm for estimating maximum-likelihood phylogenies. Mol. Biol. Evol. *32*, 268–274.

111. Stamatakis, A. (2014). RAxML version 8: a tool for phylogenetic analysis and post-analysis of large phylogenies. Bioinformatics *30*, 1312–1313.

112. Schubert, M., Lindgreen, S., and Orlando, L. (2016). AdapterRemoval v2: rapid adapter trimming, identification, and read merging. BMC Res. Notes *9*, 88.

113. Rambaut, A., Drummond, A.J., Xie, D., Baele, G., and Suchard, M.A. (2018). Posterior summarization in Bayesian phylogenetics using Tracer 1.7. Syst. Biol. *67*, 901–904.

114. Yu, G., Smith, D.K., Zhu, H., Guan, Y., and Lam, T.T.-Y. (2017). GGTREE: an R package for visualization and annotation of phylogenetic trees with their covariates and other associated data. Methods Ecol. Evol. *8*, 28–36.

115. Larsson, A. (2014). AliView: a fast and lightweight alignment viewer and editor for large datasets. Bioinformatics *30*, 3276–3278.

116. Knapas, M.T. (1987). Den medeltida kyrkan i Borgå, forskningsrön och nya alternativ. Finskt Museum, 64–86.

117. Salo, K.H. (2016). Health in Southern Finland: bioarchaeological analysis of 555 skeletons excavated from nine cemeteries (11th-19th century AD). PhD thesis (University of Helsinki).

118. Hiekkanen, M. (2003). Suomen kivikirkot keskiajalla (Otava).

119. Pihlman, S. (1992). Begravningar i Åbo under slutet av 1500-talet och början av 1600-talet, Tolkningsproblem kring Helgeandskyrkans gravar. Finskt Museum, 59–99.

120. Pinhasi, R., Fernandes, D., Sirak, K., Novak, M., Connell, S., Alpaslan-Roodenberg, S., Gerritsen, F., Moiseyev, V., Gromov, A., Raczky, P., et al. (2015). Optimal ancient DNA yields from the inner ear part of the human petrous bone. PLoS ONE *10*, e0129102.

121. Översti, S., Majander, K., Salmela, E., Salo, K., Arppe, L., Belskiy, S., Etu-Sihvola, H., Laakso, V., Mikkola, E., Pfrengle, S., et al. (2019). Human mitochondrial DNA lineages in Iron-Age Fennoscandia suggest incipient admixture and eastern introduction of farming-related maternal ancestry. Sci. Rep. *9*, 16883.

122. Ascough, P., Cook, G., and Dugmore, A. (2005). Methodological approaches to determining the marine radiocarbon reservoir effect. Prog. Phys. Geogr. *29*, 532–547.

123. Longin, R. (1971). New method of collagen extraction for radiocarbon dating. Nature *230*, 241–242.

124. Berglund, B.E., Hakansson, S., and Lagerlund, E. (1976). Radiocarbon-dated mammoth (*Mammuthus primigenius* Blumenbach) finds in South Sweden. Boreas *5*, 177–191.

125. van Klinken, G.J. (1999). Bone collagen quality indicators for palaeodietary and radiocarbon measurements. J. Archaeol. Sci. *26*, 687–695.

126. Slota, P.J., Jull, A.J.T., Linick, T.W., and Toolin, L.J. (1987). Preparation of small samples for ^{14}C accelerator targets by catalytic reduction of CO. Radiocarbon *29*, 303–306.

127. Palonen, V., Pesonen, A., Herranen, T., Tikkanen, P., and Oinonen, M. (2013). HASE–The Helsinki adaptive sample preparation line. Nucl. Instrum. Methods Phys. Res. B *294*, 182–184.

128. Tikkanen, P., Palonen, V., Jungner, H., and Keinonen, J. (2004). AMS facility at the University of Helsinki. Nucl. Instrum. Methods Phys. Res. B *223-224*, 35–39.

129. Fernandes, R., Millard, A.R., Brabec, M., Nadeau, M.-J., and Grootes, P. (2014). Food reconstruction using isotopic transferred signals (FRUITS): a Bayesian model for diet reconstruction. PLoS ONE *9*, e87436.

130. Bronk Ramsey, C., Higham, T.F.G., Brock, F., Baker, D., and Ditchfield, P. (2009). Radiocarbon dates from the Oxford AMS system: archaeometry datelist 33. Archaeometry *51*, 323–349.

131. Reimer, P.J., Reimer, R.W., and Blaauw, M. (2013). Radiocarbon dating | Calibration of the ^{14}C record. In Encyclopedia of Quaternary Science, Second Edition (Elsevier), pp. 345–352.

132. Dabney, J., Knapp, M., Glocke, I., Gansauge, M.-T., Weihmann, A., Nickel, B., Valdiosera, C., García, N., Pääbo, S., Arsuaga, J.-L., and Meyer, M. (2013). Complete mitochondrial genome sequence of a Middle Pleistocene cave bear reconstructed from ultrashort DNA fragments. Proc. Natl. Acad. Sci. USA *110*, 15758–15763.

133. Kircher, M., Sawyer, S., and Meyer, M. (2012). Double indexing overcomes inaccuracies in multiplex sequencing on the Illumina platform. Nucleic Acids Res. *40*, e3.

134. Gansauge, M.-T., and Meyer, M. (2014). Selective enrichment of damaged DNA molecules for ancient genome sequencing. Genome Res. *24*, 1543–1549.

135. Gansauge, M.-T., and Meyer, M. (2013). Single-stranded DNA library preparation for the sequencing of ancient or damaged DNA. Nat. Protoc. *8*, 737–748.

136. DePristo, M.A., Banks, E., Poplin, R., Garimella, K.V., Maguire, J.R., Hartl, C., Philippakis, A.A., del Angel, G., Rivas, M.A., Hanna, M., et al. (2011). A framework for variation discovery and genotyping using next-generation DNA sequencing data. Nat. Genet. *43*, 491–498.

137. Johnson, M., Zaretskaya, I., Raytselis, Y., Merezhuk, Y., McGinnis, S., and Madden, T.L. (2008). NCBI BLAST: a better web interface. Nucleic Acids Res. *36*, W5–W9.

138. Strimmer, K., and von Haeseler, A. (1997). Likelihood-mapping: a simple method to visualize phylogenetic content of a sequence alignment. Proc. Natl. Acad. Sci. USA *94*, 6815–6819.

139. Strimmer, K., and Rambaut, A. (2002). Inferring confidence sets of possibly misspecified gene trees. Proc. Biol. Sci. *269*, 137–142.

140. Kumar, S., Stecher, G., and Tamura, K. (2016). MEGA7: molecular evolutionary genetics analysis version 7.0 for bigger datasets. Mol. Biol. Evol. *33*, 1870–1874.

141. Centurion-Lara, A., LaFond, R.E., Hevner, K., Godornes, C., Molini, B.J., Van Voorhis, W.C., and Lukehart, S.A. (2004). Gene conversion: a mechanism for generation of heterogeneity in the tprK gene of Treponema pallidum during infection. Mol. Microbiol. *52*, 1579–1596.

142. LaFond, R.E., Centurion-Lara, A., Godornes, C., Van Voorhis, W.C., and Lukehart, S.A. (2006). TprK sequence diversity accumulates during infection of rabbits with Treponema pallidum subsp. pallidum Nichols strain. Infect. Immun. *74*, 1896–1906.

143. Centurion-Lara, A., Giacani, L., Godornes, C., Molini, B.J., Brinck Reid, T., and Lukehart, S.A. (2013). Fine analysis of genetic diversity of the tpr gene family among treponemal species, subspecies and strains. PLoS Negl. Trop. Dis. *7*, e2222.

144. Strouhal, M., Mikalová, L., Haviernik, J., Knauf, S., Bruisten, S., Noordhoek, G.T., Oppelt, J., Čejková, D., and Šmajs, D. (2018). Complete genome sequences of two strains of Treponema pallidum subsp. pertenue from Indonesia: Modular structure of several treponemal genes. PLoS Negl. Trop. Dis. *12*, e0006867.

145. Addetia, A., Tantalo, L.C., Lin, M.J., Xie, H., Huang, M.-L., Marra, C.M., and Greninger, A.L. (2020). Comparative genomics and full-length Tprk profiling of Treponema pallidum subsp. pallidum reinfection. PLoS Negl. Trop. Dis. *14*, e0007921.

146. Fieldsteel, A.H., Stout, J.G., and Becker, F.A. (1979). Comparative behavior of virulent strains of Treponema pallidum and Treponema

pertenue in gradient cultures of various mammalian cells. Infect. Immun. *24*, 337–345.

147. Hampp, E.G. (1951). Preservation of viability and pathogenicity of the Nichols' rabbit strain of Treponema pallidum by freeze drying. Public Health Rep. *66*, 501–506.

148. Sandok, P.L., Knight, S.T., and Jenkin, H.M. (1976). Examination of various cell culture techniques for co-incubation of virulent Treponema pallidum (Nichols I strain) under anaerobic conditions. J. Clin. Microbiol. *4*, 360–371.

149. Navascués, M., Depaulis, F., and Emerson, B.C. (2010). Combining contemporary and ancient DNA in population genetic and phylogeographical studies. Mol. Ecol. Resour. *10*, 760–772.

150. Rieux, A., and Balloux, F. (2016). Inferences from tip-calibrated phylogenies: a review and a practical guide. Mol. Ecol. *25*, 1911–1924.

151. Murray, G.G.R., Wang, F., Harrison, E.M., Paterson, G.K., Mather, A.E., Harris, S.R., Holmes, M.A., Rambaut, A., and Welch, J.J. (2016). The effect of genetic structure on molecular dating and tests for temporal signal. Methods Ecol. Evol. *7*, 80–89.

152. Hasegawa, M., Kishino, H., and Yano, T. (1985). Dating of the human-ape splitting by a molecular clock of mitochondrial DNA. J. Mol. Evol. *22*, 160–174.

153. Yang, Z. (1994). Maximum likelihood phylogenetic estimation from DNA sequences with variable rates over sites: approximate methods. J. Mol. Evol. *39*, 306–314.

154. Drummond, A.J., Rambaut, A., Shapiro, B., and Pybus, O.G. (2005). Bayesian coalescent inference of past population dynamics from molecular sequences. Mol. Biol. Evol. *22*, 1185–1192.

155. Drummond, A.J., Ho, S.Y.W., Phillips, M.J., and Rambaut, A. (2006). Relaxed phylogenetics and dating with confidence. PLoS Biol. *4*, e88.

156. Andrades Valtueña, A., Mittnik, A., Key, F.M., Haak, W., Allmäe, R., Belinskij, A., Daubaras, M., Feldman, M., Jankauskas, R., Janković, I., et al. (2017). The Stone Age plague and its persistence in Eurasia. Curr. Biol. *27*, 3683–3691.e8.

157. Radolf, J.D., and Kumar, S. (2018). The Treponema pallidum outer membrane. Curr. Top. Microbiol. Immunol. *415*, 1–38.

158. Bouckaert, R., Heled, J., Kühnert, D., Vaughan, T., Wu, C.-H., Xie, D., Suchard, M.A., Rambaut, A., and Drummond, A.J. (2014). BEAST 2: a software platform for Bayesian evolutionary analysis. PLoS Comput. Biol. *10*, e1003537.

STAR★METHODS

KEY RESOURCES TABLE

REAGENT or RESOURCE	SOURCE	IDENTIFIER
Chemicals, Peptides, and Recombinant Proteins		
EDTA solution, pH 8.0, 0.5 M	AppliChem	Cat#A4892,1000
1x Tris-EDTA pH 8.0	AppliChem	Cat#A8569,0500
Proteinase K, Molecular Biology Grade, 1600 Units	BioConcept AG	Cat#P8107S
Guanidine hydrochloride	Sigma-Aldrich	Cat#G3272-500 g
3M Sodium Acetate pH 5.5	Sigma-Aldrich	Cat#S7899-500ML
Ethanol	Merck	Cat#1009832511
Isopropanol	Merck	Cat#1070222511
BSA Molecular Biology Grade (conc. 20 mg/ml), 12 mg	BioConcept AG	Cat#B9000S
Adenosine 5′-Triphosphate (ATP), 1 ml	BioConcept AG	Cat#P0756S
Bst 2.0 DNA Polymerase, 1600 units	BioConcept AG	Cat#M0275S
dNTPs 25 mM	Thermo Scientific	Cat#R1121
Quick Ligation Kit, 150 reactions	BioConcept AG	Cat#M2200L
T4 DNA Polymerase, 150 units	BioConcept AG	Cat#M0203S
T4 Polynucleotide Kinase, 500 units	BioConcept AG	Cat#M0201S
PfuTurbo Cx Hotstart DNA POL, 1000 U	Agilent Technologies	Cat#600414
Tween 20	Sigma-Aldrich	Cat#P9416-50ML
User Enzyme, 250 units	BioConcept AG	Cat#M5505 L
Water Molecular grade	Sigma-Aldrich	Cat#W4502-1L
Water Chromasolv Plus for HPLC	Sigma-Aldrich	Cat#34877-2.5L
PB-Buffer	QIAGEN	Cat#19066
NEB Buffer 2 (10X)	BioConcept AG	Cat#B7002S
Isothermal Buffer (10x)	BioConcept AG	Cat#B0537S
NaCl solution, 5 M	Sigma-Aldrich	Cat#S5150-1L
SDS solution, 20%	Ambion	Cat#AM9820
SSC buffer, 20X	Ambion	Cat#AM9770
Tris-HCl solution, pH 8, 1M	AppliChem	Cat#A4577,0500
FastAP thermosensitive alkaline phosphatase	ThermoScientific	Cat#EF0651
PEG-4000 solution, 50% (wt/vol)	Sigma-Aldrich	Cat#89782-100ML-F
Dynabeads MyOne streptavidin C1	Life Technologies	Cat#65001
dNTP mix 25mM each	ThermoScientific	Cat#R1121
T4 DNA Polymerase	ThermoScientific	Cat#EP0062
T4 DNA Ligase	ThermoScientific	Cat#EL0012
pUC19	NEB	Cat#N3041S
T4 DNA Ligase, HC (30 U/μL)	ThermoScientific	Cat#EL0013
T4 DNA Ligase (5 U/μL)	ThermoScientific	Cat#EL0012
T4 RNA Ligase Reaction Buffer	BioConcept AG	Cat#B0216L
DNA Polymerase I, Large (Klenow) Fragment (5000U/ml)	BioConcept AG	Cat#M0210L
T4 Polynucleotide Kinase (10U/μl)	ThermoScientific	Cat#EK0032
ATP Solution (100 mM)-0.25 mL	Thermo Fisher / Life Technologies Europe BV	Cat#R0441
Klenow Fragment (10 U/μL)-1,500 units	Thermo Fisher / Life Technologies Europe BV	Cat#EP0052
Agilent Oligo aCGH/Chip-on-Chip Wash Buffer 2, 4L	Agilent	Cat#5188-5222

(*Continued on next page*)

Continued

REAGENT or RESOURCE	SOURCE	IDENTIFIER
Oligo aCGGH/Chip-onchip Hybridization Kit	Agilent	Cat#5188-5220
Oligo aCGH/ChIP-on-chip Wash Buffer Kit	Agilent	Cat#5188-5226
Agilent Oligo aCGH/Chip-on-Chip Wash Buffer 1, 4L	Agilent	Cat#5188-5221
Amplitaq Gold Kit 1000U mit Puffer + MgCl2	Applied	Cat#4311816
Critical Commercial Assays		
Zymo-Spin V Columns w/ Reservoir	Lucerna Chem AG - Cat.1	Cat#ZYM-C1016-50-50ST
Min Elute PCR Purification Kit	QIAGEN	Cat#28006
SYBR Green PCR Master Mix-2 × 5 mL	Thermo Fisher / Life Technologies Europe BV - Kernsortiment	Cat#4364344
Herculase II Fusion DNA POL, 400 rxn	Agilent Technologies (Schweiz) AG	Cat#600679
D1000 Reagents for 112 samples	Agilent Technologies (Schweiz) AG	Cat#5067-5583
D1000 ScreenTape for 112 samples	Agilent Technologies (Schweiz) AG	Cat#5067-5582
DNA1000 Lab Chip Kit	Agilent	Cat#5067-1504
SureSelect DNA Capture Arrays 1M	Agilent Technologies	Cat#046466
Deposited Data		
T. pallidum aDNA raw data	This study	ENA: PRJEB35855, https://www.ebi.ac.uk/ena/data/view/PRJEB35855
Oligonucleotides		
IS1_adapter.P5 A*C*A*C*TCTTTCCCTACACGACGC TCTTCCG*A*T*C*T	[98]	Sigma Aldrich
IS2_adapter.P7 G*T*G*A*CTGGAGTTCAGACGTGT GCTCTTCCG*A*T*C*T	[98]	Sigma Aldrich
IS3_adapter.P5+P7 A*G*A*T*CGGAA*G*A*G*C	[98]	Sigma Aldrich
IS 7_Short_amp_P5 ACACTCTTTCCCTACACGAC	[98]	Sigma Aldrich
IS 8_short_amp_P7 GTGACTGGAGTTCAGACGTGT	[98]	Sigma Aldrich
IS 5_Reamp_P5 AATGATACGGCGACCACCGA	[98]	Sigma Aldrich
IS 6_Reamp_P7 CAAGCAGAAGACGGCATACGA	[98]	Sigma Aldrich
B04_Blocking Primer GTGACTGGAGTTCAGACGTGTG CTCTTCCGATCT-Phosphat	[98]	Sigma Aldrich
B06_Blocking Primer CAAGCAGAAGACGGCATACGA GAT-Phosphat	[98]	Sigma Aldrich
B08_Blocking Primer GTGTAGATCTCGGTGGTCGCC GTATCATT-Phosphat	[98]	Sigma Aldrich
B10_Blocking Primer GGAAGAGCGTCGTGTAGGGA AAGAATGT-Phosphat	[98]	Sigma Aldrich
B11_Blocking Primer GGAAGAGCGTCGTGTAGGGAA AGAATGT[Phos]	[98]	Sigma Aldrich
Fwd index primer (Extention Primer with Index) CAAG CAGAAGACGGCATACGAGAT-INDEX-GTGACTGGAGTTCAGACGTGT	[98]	Sigma Aldrich
Rvs index Primer (Extention Primer with Index) AATGA TACGGCGACCACCGAGATCTACAC-INDEX-ACACTCTTTCCCTACACGACGCTCTT	[98]	Sigma Aldrich
Software and Algorithms		
EAGER	[69]	https://github.com/apeltzer/EAGER-GUI
MarkDuplicates (Picard) v2.15.0	[99]	http://broadinstitute.github.io/picard/; RRID: SCR_006525

(*Continued on next page*)

Continued

REAGENT or RESOURCE	SOURCE	IDENTIFIER
MapDamage v.2.0	[100]	https://ginolhac.github.io/mapDamage/; RRID: SCR_001240
GATK UnifiedGenotyper v.3.8.0	[101]	https://software.broadinstitute.org/gatk/; RRID: SCR_001876
MultiVCFAnalyzer	[102]	https://github.com/alexherbig/MultiVCFAnalyzer
BEAST2 v.2.6	[82]	https://www.beast2.org/; RRID: SCR_017307
BEDtools	[103]	http://bedtools.readthedocs.io/en/latest/; RRID: SCR_006646
ggplot2	[104, 105]	http://ggplot2.org/; RRID: SCR_014601
RStudio	[106]	https://rstudio.com/; RRID: SCR_000432
Circleator	[56]	https://github.com/jonathancrabtree/Circleator/; RRID: SCR_002801
SNPEvaluation	[107, 108]	https://github.com/andreasKroepelin/SNP_Evaluation
FastQC	[109]	https://github.com/s-andrews/FastQC/releases; RRID: SCR_014583
IQ-TREE v.1.6.10	[110]	http://www.iqtree.org/
RaxML v. 8.2.12	[111]	https://github.com/stamatak/standard-RAxML
CircularMapper v.1.0	[69]	https://github.com/apeltzer/CircularMapper
AdapterRemoval v.2.2.1	[112]	https://github.com/MikkelSchubert/adapterremoval; RRID: SCR_011834
Tracer v1.7	[113]	http://beast.community/tracer
ggtree	[114]	https://bioconductor.org/packages/release/bioc/html/ggtree.html
AliView 1.21	[115]	https://github.com/AliView
Other		
T. pallidum colonial Mexican aDNA	[52]	ENA: RJEB21276, https://www.ebi.ac.uk/ena/data/view/PRJEB21276
Modern T. pallidum genome set	[41]	SRA: PRJNA313497, https://www.ncbi.nlm.nih.gov/bioproject/?term=PRJNA313497
T. pallidum DAL_1 genome	[71]	GenBank: CP003115.1, https://www.ncbi.nlm.nih.gov/nuccore/CP003115
T. pallidum Nichols genome	[75]	GenBank: NC_021490.2, https://www.ncbi.nlm.nih.gov/nuccore/NC_021490.2
T. pallidum Chicago genome	[70]	GenBank: NC_017268.1, https://www.ncbi.nlm.nih.gov/nuccore/NC_017268.1
T. pallidum SEA81_4 genome	[77]	GenBank: CP003679.1, https://www.ncbi.nlm.nih.gov/nuccore/CP003679.1
T. pallidum P3 genome	[78]	SRA: SRR2996731, https://trace.ncbi.nlm.nih.gov/Traces/sra/?run=SRR2996731
T. pallidum SS14 genome	[75]	GenBank: NC_021508.1, https://www.ncbi.nlm.nih.gov/nuccore/NC_021508.1
T. pallidum Mexico A genome	[73]	GenBank: NC_018722.1, https://www.ncbi.nlm.nih.gov/nuccore/NC_018722.1
T. pallidum Fribourg-Blanc genome	[74]	GenBank: NC_021179.1, https://www.ncbi.nlm.nih.gov/nuccore/NC_021179.1
T. pallidum Gauthier genome	[72]	GenBank: NC_016843.1, https://www.ncbi.nlm.nih.gov/nuccore/NC_016843.1
T. pallidum CDC2 genome	[72]	GenBank: NC_016848.1, https://www.ncbi.nlm.nih.gov/nuccore/NC_016848.1
T. pallidum Samoa D genome	[72]	GenBank: NC_016842.1, https://www.ncbi.nlm.nih.gov/nuccore/NC_016842.1

(*Continued on next page*)

Continued

REAGENT or RESOURCE	SOURCE	IDENTIFIER
T. pallidum Bosnia A genome	[76]	SRA: SRR3268694, https://www.ncbi.nlm.nih.gov/sra/SRR3268694
T. pallidum PT_SIF1002 genome	Unpublished data	GenBank: NZ_CP016051.1, https://www.ncbi.nlm.nih.gov/nuccore/NZ_CP016051.1

RESOURCE AVAILABILITY

Lead Contact

Additional information and requests for resources and reagents should be directed to and will be fulfilled by the Lead Contact, Verena J. Schuenemann (verena.schuenemann@iem.uzh.ch).

Materials Availability

This study did not generate new unique reagents.

Data and Code Availability

The accession number for the data reported in this paper is ENA: PRJEB35855. The original datasets and code generated during this study are available at DOI: https://doi.org/10.5281/zenodo.3925826. The workflow and scripts for molecular clock dating and date randomisation tests are additionally available at https://github.com/laduplessis/Treponema_pallidum_in_early_modern_Europe.

EXPERIMENTAL MODEL AND SUBJECT DETAILS

Ethical approvals

All ancient human remains used in this study come from archaeological excavations and are over 100 years old. Therefore, they are not subject to the Human Tissue Act (2004) and no ethics approvals are required.

Description of archaeological contexts and sample selection

Porvoo Cathedral burial ground

The stone Dome of Porvoo in Finland gained its status as a Cathedral in 1723 [116], although an earlier, wooden church has been on the site, and the cemetery around it used likely as early as 13th to 14th century on. However, most of the individuals excavated from the site in 2007 were buried in a 17th to 18th century style in coffins, and were relatively wealthy, considering their burial location at the prestigious, southern side of the church. The late timescale is confirmed by the lower bound of the radiocarbon dating of the PD28 individual in 1666 CE, although the upper bound reaches into the modern era (Klaus-Tschira-Archäometrie-Zentrum am Curt-Engelhorn-Zentrum, Mannheim, Germany: MAMS 35328, Figure S1). It is known that the cemetery was formally used until 1789, and the churchyard leveled in 1791, providing a historical limit to date the remains excavated from the site [117,118] .

The Holy Ghost Chapel, Turku

Historical Julin's plot in Turku, Finland, contained the Church of the Holy Ghost and its cemetery. It was also a location of an early hospital for the poor (House of the Holy Ghost). The cemetery was used over at least two hundred years, from the end of the 14th century to the mid-17th century [119]. The remains excavated from the site in 1985 were deposited in the crypt of the Holy Ghost Chapel, located in the Casagrande property later built on the plot. The radiocarbon dating for the individual CHS119 placed the bone material between the years 1443 and 1460 CE (Klaus-Tschira-Archäometrie-Zentrum am Curt-Engelhorn-Zentrum, Mannheim, Germany: MAMS 35325), but the reservoir effect corrections calculated at the Helsinki Natural History Museum Laboratory of Chronology revealed a dual peak pattern of two time windows, one between 1450 and 1525 CE, and another between 1570 and 1630 CE [57, 58] (Figure S1).

St Jacob's cemetery, Tartu

St. Jacob's suburban cemetery in Tartu is archaeologically dated to from the 13th to late 16th centuries. The suburban cemetery was used by lower social strata. Independent radiocarbon dating analyses for the individual SJ219 were produced in two laboratories (Klaus-Tschira-Archäometrie-Zentrum am Curt-Engelhorn-Zentrum, Mannheim, Germany: MAMS 35326 and the AMS laboratory, ETH Zürich: ETH-100446), both of which place the individual in the 15th century (1434-1446 and 1429-1476 CE, respectively, Figure S1). In addition to the bone of individual SJ219, a preserved fragment from her wooden coffin was dated in order to estimate a date that would not be affected by any potential dietary reservoir effect (AMS laboratory, ETH Zürich: ETH-101915). Unfortunately, this dating provided a wider temporal range than that of the human remains from the grave (1463 to 1635 CE). The upper boundary of the wood sample dating was chosen as an upper limit in the BEAST2 analyses to avoid bias from the possible reservoir effect in the bone material.

Gertrude's Infirmary, Kampen

The Kampen sample KM14-7 was radiocarbon dated to 1494-1631 CE (Klaus-Tschira-Archäometrie-Zentrum am Curt-Engelhorn-Zentrum, Mannheim, Germany: MAMS 33918, Figure S1). The sample stems from a collection of disarticulated skeletal material found in a large excavated area within the cemetery of Gertrude's Infirmary in Kampen, the Netherlands. The use of this graveyard

spans from the mid-14th to early 17th century. Reservoir effect corrections are not planned at this time. It is, however, noted from the stable isotope values ($\delta^{15}N$ and $\delta^{13}C$) in the bone material, that a marine reservoir effect due to the individual's diet could possibly affect the radiocarbon dates retrieved for the sample.

Altogether nine individuals from Estonian, Finnish and Netherlandic sources were tested for treponemal DNA. (The list of included samples: Porvoo Dome, Porvoo, Finland: grave 28, petrous part of temporal bone; St. Jacob's Cemetery, Tartu, Estonia: individual 219, phalanx and premolar; St. Georges' Cemetery, Tartu, Estonia: individual 34, metacarpal bone and premolar; Holy Ghost Chapel, Turku Finland: individuals 101, molar; 107, molar; 119, premolar; 122, molar; 305, molar; and Gertrude's Infirmary, Kampen, the Netherlands: individual 14, disintegrated tibia fragment N:o 7). Samples confirmed to be positive for the treponemal agent's DNA included the perinatal individual's petrous bone from Porvoo, Finland (PD28), the premolar from Turku, Finland (CHS119), the metacarpal bone from Tartu, Estonia (SJ219), and the fragment of tibia from Kampen, the Netherlands (KM14-7). The skeletal elements were chosen either due to the visible lesions, or to the individual's perinatal death, indicating a possible congenital case of syphilis. A petrous portion of the skull was used for the perinatal individual from Porvoo, as it is generally the most well-preserved part of the skeleton [120]. Since congenital syphilis is considered to be systemic [96], we expected all of the skeletal elements of this individual to be affected by the potential infection. All the five individuals tested from Turku showed signals of treponemal infection: mulberry molars, bone changes in the skull or lesions in the long bones. The Turku individuals were previously studied for their mitochondrial human DNA and published in a population genetics study [121]. The individuals from the two Tartu sites, St. Jacobs cemetery and St. George's cemetery, were both studied archaeologically and, showing signs of severe infection which affected their skeleton, they were chosen to be tested for treponemal diseases. The Kampen individual is represented by only one fragmented tibia, found disarticulated from the burial ground at the excavation of Gertrude's Infirmary. The tibia had a periosteal lesion of striated woven bone, also causing a bowing of the bone, which indicates possible treponemal infection in the individual.

METHOD DETAILS

Sample processing

Documentation and UV-irradiation of the bone material for decontamination, as well as laboratory procedures for sampling, DNA extraction, library preparation and library indexing were all conducted in facilities dedicated to ancient DNA work at the University of Tübingen, with necessary precautions taken including protective clothing and minimum contamination-risk working methods.

All post-amplification steps were performed in a laboratory provided by the Department of Toxicology at the University of Tübingen as well as in the post-PCR laboratory of the Paleogenetics Group, Institute of Evolutionary Medicine (IEM), University of Zurich (UZH). DNA sequencing was performed at the sequencing facilities of the Max Planck Institute for the Science of Human History in Jena or at the Functional Genomics Center at the University of Zurich (FGCZ).

Reservoir effect correction of the CHS119 sample

Marine and freshwater reservoir effects can cause an offset in C^{14} ages between contemporaneous remains of humans or animals, depending on whether they relied mainly on terrestrial or aquatic food sources [122]. The protocols for radiocarbon dating and stable isotopic measurements for CHS119 sample at the Laboratory of Chronology, Finnish Natural History Museum, were as follows. The method for collagen extraction was based on the Longin method [123] and followed a previously described protocol by Berglund and colleagues [124]. To check post-mortem alteration, the contents of N and C (wt-%) and the atomic C/N ratio of the collagen were monitored (C-% = 37.4%, N-% = 13.6%, C/N ratio = 3.2) fulfilling the accepted quality criteria for well-preserved collagen i.e., 2.9–3.6 [125].

For radiocarbon analysis, the collagen sample was packed inside a silver cup (Elemental Microanalysis D2001) and the packed sample was combusted with an Elemental Analyzer (Thermo Scientific Flash 2000 NC). The resulting CO_2 was cryogenically trapped and reduced to graphite in the presence of zinc powder and iron catalyst [126] by using the Labview controlled HASE facility [127]. The graphite sample was measured for radiocarbon contents at the Helsinki AMS facility [128]. The result has been normalized for isotopic fractionation by using the $\delta^{13}C$ value measured with the AMS facility. Lastly, the radiocarbon date (HeLa-4271) of 383 ± 24 BP was obtained.

Dietary stable isotopic (carbon and nitrogen) ratios were measured from bone collagen parallel to AMS analyses for the sample CHS119 at the Finnish Natural History Museum facility by using EA-IRMS technique. The elemental content and isotopic composition of carbon and nitrogen were measured on a NC2500 elemental analyzer coupled to a Thermo Scientific Delta V Plus isotope ratio mass spectrometer. The raw isotope data were normalized with a two-point calibration using international reference materials with known isotopic compositions (USGS-40, USGS-41). The mean measured raw $\delta^{13}C$ and $\delta^{15}N$ values for calibration references were -26.7 and -4.7 for USGS-40 and 36.2 and 46.5 for USGS-41, respectively. Replicate analyses of a quality control reference analyzed alongside the unknowns indicate a 1σ internal precision of ≤ 0.1 for both $\delta^{13}C$ and $\delta^{15}N$. This process resulted in dietary isotopic values of $\delta^{13}C = -19.7‰$ and $\delta^{15}N = 12.3‰$.

To obtain an estimate for a potential reservoir effect (RE) within the radiocarbon age, dietary modellings with FRUITS software [129] were performed based on an assumption of three food groups (marine, freshwater and terrestrial foods), and adopting the macronutrient concentrations, isotopic offsets and the isotopic baseline data [58] from the δIANA database [57] was used for gathering the Northern European isotopic data. The marine isotopic signature and corresponding marine reservoir effect was assumed to come from the vicinity of Finland Proper (Bothnian Sea, Archipelago and its surroundings). It was estimated [58] that this corresponds

to the maximal marine reservoir effect (in marine animals) of 173 ± 41 ^{14}C years. The dietary modeling provided the contribution of bone collagen carbon from such a source and provided means to scale down the potential reservoir age of human bone collagen. Correspondingly, the maximal freshwater reservoir effect (in fish) was estimated as 107 ± 52 ^{14}C years. Eventually, the human bone collagen REs was estimated to be MRE = 28 ± 11 ^{14}C years and FRE = 11 ± 9 ^{14}C years yielding to a RE-corrected radiocarbon age of 345 ± 29 ^{14}C years corresponding to the HeLa-4271 measurement. As the same amount of RE is also assumed for MAMS-35325 measurement (421 ± 18 BP), the same correction was adopted yielding to 383 ± 24 ^{14}C years. Finally, the combined RE-corrected radiocarbon age of 368 ± 19 ^{14}C years was obtained. These ages were calibrated according to Bronk Ramsey et al. [130] and Reimer et al. [131] (Figure S1).

Sampling and DNA extraction

Before extracting DNA from the samples, all surfaces were irradiated with ultraviolet light (UV-irradiated) to minimize potential contamination from modern DNA. DNA extraction was performed according to a well-established extraction protocol for ancient DNA [132]. For DNA extraction, 30-120 mg of bone powder was used per sample. The bone powder was obtained by drilling bone tissue using a dental drill and dental drill bits. For different individuals, variable amounts of extracts were produced. During each extraction, one positive control (ancient cave bear bone powder sample) and one negative control were included for every ten samples. Positive extraction controls were carried along until the indexing of DNA-libraries, and the negative controls were carried through all following experiments and sequenced.

Library preparation

In this study, double-stranded (ds) and single-stranded (ss) DNA-libraries were produced. All DNA library preparation procedures applied in this study are described in the following paragraphs.

Double-stranded DNA library preparation

For the preparation of DNA-libraries 20μl of DNA extract was converted into ds-DNA libraries [133]. For every ten libraries produced, one negative control was used. Negative controls for library preparations were processed in parallel with all following experiments. Sample-specific barcodes (indexes) were added to both ends of the libraries [98]. The indexed libraries were then amplified to reach a minimum DNA concentration of 90ng/μl. The amplification was performed using 1x Herculase II buffer, 0.4 μM IS5 and 0.4 μM IS6 primer [98], Herculase II Fusion DNA Polymerase (Agilent Technologies), 0.25 mM dNTPs (100 mM; 25 mM each dNTP) and 5 μl indexed library as DNA template. Four reactions per library were prepared and the total amplification reaction volume was 100μl. The thermal profile included an initial denaturation for 2 minutes at 95°C and 3-18 cycles, depending on DNA concentration after indexing of the libraries, denaturation for 30 s at 95°C, 30 s annealing at 60°C and a 30 s elongation at 72°C, followed by a final elongation step for 5 minutes at 72°C. All splits of one indexed library were pooled and purified using the QIAGEN MinElute PCR purification kit. The final quantification for all DNA libraries was performed with the Agilent 2100 Bioanalyzer.

Uracil-DNA Glycosylase (UDG) treated double-stranded DNA library preparation

To avoid potential sequencing artifacts caused by the characteristic ancient DNA damage profile [134] additional libraries for genome-wide enrichment were created, namely 30μl of DNA extract was pre-treated with uracil-DNA glycosylase [62]. Controls were also treated accordingly. Sequencing libraries were indexed and amplified as described above.

Single-stranded DNA library preparation

Single-stranded libraries were generated from 20 μL of DNA extract according to established protocols [135]. Two single-stranded libraries were prepared for the four positive individuals. All single-stranded libraries were indexed and amplified with the same experimental procedures as applied and described for the double-stranded DNA libraries. To assess the library concentration, D1000 High Sensitivity ScreenTape was used on an Agilent 2200 Tapestation. All libraries were pooled in equimolar concentration for the genome-wide enrichment step.

Capture techniques

Capture for a first screening for treponemal DNA

For the first screening for *Treponema pallidum* DNA, all double-stranded libraries without UDG treatment for all individuals were pooled. All negative controls were pooled separately. The *T. pallidum* screening was performed using a modified version [41] of the array capture approach originally developed by Hodges and colleagues [59] to enrich the sample libraries for *T. pallidum*-specific DNA. Here, we used arrays designed by Agilent Technology and the blocking oligonucleotides (BO) 4, 6, 8, and 10 [98] in the initial screening and followed the same enrichment procedure as described by Arora and colleagues [41] and Schuenemann and colleagues [52], as follows:

Whole-genome capture

After the analysis of the shotgun screening data from the initial sequencing, UDG-treated double-stranded DNA libraries and single-stranded DNA libraries were produced for samples potentially positive for syphilis and used for whole genome capture. The whole-genome capture was performed as described above using the same array enrichment strategy. In addition to the blocking oligonucleotides for double-stranded libraries, specific blocking oligonucleotides 4, 6, 8, and 11 [98] were used for single-stranded

libraries. The whole-genome enrichment for treponemal DNA was produced in three rounds of array capture and a maximum of two libraries from different individuals were pooled for each array. Enrichment pools were diluted to 10 nMol/L for sequencing.

In-solution capture for KM14-7

An additional in-solution capture procedure was performed for sample KM14-7 to obtain higher coverage. Genome-wide enrichment of single-stranded libraries was performed through custom target enrichment kits (Arbor Bioscience). RNA baits with a length of 60 nucleotides and a 4bp tiling density were designed based on three reference genomes (Nichols, GenBank: CP004010.2, SS14: GenBank CP000805.1, Fribourg Blanc: GenBank CP003902). Five hundred ng library pools were enriched according to the manufacturer's instructions. Captured libraries were amplified in 3 × 100 μL reactions containing 1 unit Herculase II Fusion DNA polymerase (Agilent), 1x Herculase II reaction buffer, 0.25mM dNTPs, 0.4 μM primers IS5 and IS6 [98] and 15 μL library template. The thermal profile was the following: initial denaturation at 95°C for 2 min, 14 cycles of denaturation at 95°C for 30 s, annealing at 60°C for 30 s, and elongation at 72°C for 30 s, followed by a final elongation at 72°C for 5 min. Captured libraries were purified with MinElute spin columns (QIAGEN) and quantified with a D1000 High Sensitivity ScreenTape on an Agilent 2200 TapeStation.

Sequencing

The first two rounds of genome-wide enriched (array enrichment strategy) double-stranded libraries were sequenced at the Max Planck Institute for the Science of Human History in Jena on an Illumina HiSeq 4000 platform with 1*75+8+8 cycles (single-end reads), following the manufacturer's protocols for multiplex sequencing. The third round of genome-wide array capture enrichment for *Treponema pallidum* DNA by double-stranded libraries was sequenced at the Max Planck Institute for the Science of Human History in Jena on an Illumina HiSeq 4000 platform with 2*50+8+8 cycles (paired-end reads), following manufacturer's protocols. In the fourth round of sequencing the single-stranded DNA libraries, enriched by array capture strategy for *Treponema pallidum* DNA, were sequenced. The sequencing was performed on an Illumina NextSeq500 platform 2*75+8+8 cycles (paired-end reads) at the Functional Genomics Center Zurich.

Read processing, mapping and variant calling

The data from the preliminary shotgun-sequencing of the PD28 sample and a screening capture for the samples SJ219, CHS119 and KM14-7 were used to select the four samples in this study as *T. pallidum* positive candidates. The four selected samples then underwent a subsequent enrichment targeted for the genetic sequence of *T. pallidum*. The resulting data was processed as described in the following paragraphs.

The capture data from the sequencing runs were merged sample-wise and data processing was performed using EAGER version 1.92.37 (Efficient Ancient GEnome Reconstruction) [69]. The quality of the sequencing data was assessed using the FastQC [109] and the reads were adaptor trimmed with AdapterRemoval ver. 2.2.1a [112]. Sequencing reads were mapped to a TPA Nichols reference genome (CP004010.2) using CircularMapper version 1.0 [69] with a minimum quality score of 37 and a stringency parameter n = 0.1. Duplicates were removed with MarkDuplicates v2.15.0 [99]. MapDamage version 2.0.6 [100] was used to investigate the damage patterns, which can authenticate the ancient origin of the DNA sequences (Figure S2) and Circleator plots [56] were produced to showcase the different genome coverages among the samples (Figure S3). The Genome Analysis Toolkit (GATK) version 3.8.0 [101, 136] was used to perform SNP calling and generate *vcf.* files for each genome. The same procedure was also employed after mapping reads to the TPE CDC2 genome (CP002375.1), in order to assess potential reference-related biases on the phylogenetic inference.

Genomic dataset and multisequence alignment

We constituted a genomic dataset representative of the extant diversity of *T. pallidum* and including the three previously published ancient genomes from Mexico. Raw sequencing data was gathered for strains that were high-throughput sequenced. The previously exposed procedure was then applied to obtain *vcf.* files for each genome. We used MultiVCFAnalyzer [102] to produce alignments with the following parameters: bases were called if covered by at least two reads with a mapping quality of 30 and a consensus of at least 90% (with the one-read-exception rule implemented in MultiVCFAnalyzer). The resulting alignment was realigned with already assembled genomes (isolates Bosnia A, CDC2, Chicago, Fribourg, Gauthier, Mexico A, PT_SIF1002, SS14, and SEA81_4_1), using AliView version 1.21 [115]. A complete dataset used for the phylogenetic analyses consisted of 26 modern *Treponema pallidum* strains [41, 70–78] including PT_SIF1002 (unpublished, GenBank: NZ_CP016051.1) and all ancient genomes used in this study. For the molecular dating analysis with BEAST2, two highly passaged modern strains (NIC2, Nichols) and the two ancient strains from colonial Mexico [52] (94A and 94B) along with the European ancient genome KM14-7 from this study, were excluded.

SNP quality assessment

Calling SNPs from ancient bacterial DNA data is challenging due to DNA damage, potential environmental contamination and low genome coverage which may lead to the recovery of artifactual genetic variation in reconstructed DNA sequences. This can interfere with all subsequent analyses and, in particular, lead to artificially long branches in phylogenetic trees and impede time-calibrated analyses. Artifactual SNPs resulting from environmental contamination shared between several samples may also lead to biases in inferred phylogenetic tree topologies or generate misleading evidence of genetic recombination.

In order to filter for artifactual SNPs, we used the SNPEvaluation tool [107] as proposed by Keller and colleagues [108]. To generate the required *vcf.* file for genomes generated through Sanger sequencing, we simulated NGS-like reads based on genome assemblies using the tool Genome2Reads (integrated in the EAGER pipeline [69]), which were then mapped to the Nichols and CDC2 reference

genomes according to the previously described procedure. For all newly generated ancient genomes, as well as for all previously published genomes for which the mean sequencing coverage was below 20, we reviewed all unique SNPs (Tables S1 and S2). We also reviewed any SNP shared by less than 6 genomes that had at least one of the following features in a 50-bp window around the SNP: (i) some positions were not covered, (ii) the reference was supported by at least one read or (iii) the coverage changed depending on the mapping stringency (i.e., we compared the initial alignments with "low-stringency" alignments produced with bwa parameter n = 0.01). Any SNP supported by less than four reads was excluded (i.e., N was called at that position) if at least one read supported the reference or if the SNP was "damage-like" (i.e resulting from a C to T or G to A substitution). Furthermore, the specificity of the reads supporting the SNPs was verified by mapping them against the full GenBank database with BLAST [137]. Any SNP supported by reads mapping equally or better to other organisms than *T. pallidum* was excluded. Since many of these false SNPs likely arising from non-specific mapping were located in tRNAs, we excluded all tRNAs from the alignments. The list of excluded positions was written in a gff file (Data S1) and removed from the full alignment (Data S2) generated by MultiVCFAnalyzer using an in-house bash script.

Phylogenetic and recombination analysis

An analysis pipeline described by Pla-Díaz and colleagues (M.P.-D., unpublished data) was used to investigate putative recombining genes, which could potentially interfere with phylogenetic tree topologies between the modern and ancient lineages. Altogether 12 putative recombinant genes were subsequently excluded, resulting in an alternative positioning of the ancient TPA strains close to the Nichols cluster. The pipeline included the following steps: 1) Obtaining an ML tree with the complete multiple alignment, using IQ-TREE v.1.6.10 [110]. 2) Obtaining ML trees for each protein-coding gene. 3) Testing the phylogenetic signal in each gene alignment [138]. 4) Testing the congruence between each gene tree and the complete genome alignment and between each gene alignment and the complete genome tree [139]. 5) Confirming a minimum of three consecutive SNPs congruent with a recombination event for all genes passing the filtering of step 3 and 4 using MEGA7 v. 7.0 [140]. 6) Removing the protein-coding genes with signals of being involved in recombination events.

Prior to the final phylogenetic analyses, genes containing recombining regions identified through the above-mentioned procedure were excluded from the sequence alignment (Data S3). Additionally, 18 genes previously reported as hypervariable, carrying many repetitive regions and inducing recombination-like effects in mapping were considered to potentially bias the phylogenetic signal [38, 141–145] and were also removed. Those included the *arp* gene (TPANIC_0433), *FadL* homolog genes (TPANIC_0548 TPANIC_0856, TPANIC_0858, TPANIC_0859, TPANIC_0865) and all *tpr* genes TPANIC_0009, TPANIC_0011, TPANIC_0117, TPANIC_0131, TPANIC_0313, TPANIC_0316, TPANIC_0317, TPANIC_0610, TPANIC_0620, TPANIC_0621, TPANIC_0897, TPANIC_1031). Finally, positions having > 25% missing data were trimmed, and a SNP alignment was generated, recording the number of constant sites to allow ascertainment bias correction (Data S3). A phylogenetic analysis was performed using RAxML v. 8.2.12 [111] with the rapid bootstrap algorithm. The ASC_GTRGAMMA substitution model was used together with the "stamatakis" ascertainment bias correction to account for the number of constant sites not appearing in the SNP alignment.

The same analysis was conducted on different alignments to assess the effect of data processing on phylogenetic inference (Figures S4 and S5). Using a full genome instead of a SNP alignment (Figure S4B), keeping positions with > 25% missing data (Figure S4C), or using the TPE CDC2 reference genome for read mapping (Figure 2; Data S4) had little effect on the resulting tree topology, which supports the robustness of our results with respect to these aspects of data processing. Conversely, the inclusion of recombining or the abovementioned mapping-obstructing genes in the alignment (Figures S4D and S4E) resulted in topological changes, particularly regarding the position of the PD28, SJ219, 94A and 94B ancient genomes with respect to modern TPA clades. This highlights that genetic recombination may significantly bias phylogenetic reconstruction of *Treponema* if not accounted for.

KM14-7 SNP analysis

In the phylogenetic tree, KM14-7 was placed basal to TPE and TEN clades. Although bootstrap support was very high, we further evaluated the authenticity of this remarkable position because this genome contained a large fraction of missing data. First, we conducted a phylogenetic analysis based on genomic positions that were resolved in KM14-7 only (107 SNPs after exclusion of recombining genes, *FadL* homologs, *tpr* genes and *arp* gene, as well as positions with > 25% missing data). In the resulting tree, KM14-7 was still recovered basal to TPE/TEN with strong support (Figure S4F). We then investigated genomic positions for which the ancestral variant of TPE/TEN and TPA was likely different. Our rationale was that if KM14-7's position on the branch connecting TPE/TEN and TPA was authentic, the genome should contain a significant number of both TPE/TEN and TPA-like variants. Hence, we looked at positions (i) resolved in KM14-7, (ii) for which the majority variant was differing between TPE/TEN and TPA clades, but (iii) shared by more than 90% of the (modern) genomes within each clade. We then looked at the proportion of TPE/TEN and TPA-like variants in KM14-7 and compared that with all other genomes. Because KM14-7 was not included in the recombination analysis, we did not trim the recombining regions for this analysis in order to avoid a bias.

Molecular clock dating

KM14-7 and the Mexican TPA genomes, 94A and 94B, were removed from the molecular clock dating analyses due to their low coverage and the amount of unique SNPs present on these lineages. Furthermore, the Nichols and NIC2 genomes were removed to avoid any bias caused by continuous passaging in rabbit hosts from their isolation in the clinical context in 1912 until at least 1981 [142, 146–148].

The strength of the molecular clock signal in the dataset was investigated by regressing the root-to-tip genetic distance (measured in substitutions/site) of genomes against their sampling dates [149, 150]. Root-to-tip genetic distances were calculated on a midpoint-rooted ML tree estimated in RAxML v. 8.2.11 [111] using the same procedure described above. Sampling dates of ancient sequences were fixed to the middle of the date range defined by radiocarbon dating (Table 3). To assess the significance of the correlation, we permuted the sampling dates across genomes and used the Pearson correlation coefficient as a test statistic [149, 151]. We performed 1000 replicates and calculated the p value as the proportion of replicates with a correlation coefficient greater than or equal to the truth, using the unpermuted sampling dates (Figure S5).

Divergence times and substitution rates were estimated using BEAST2 v. 2.6 [82]. Analyses were performed under an HKY substitution model with Γ-distributed rate heterogeneity [152, 153] and a Bayesian skyline plot demographic model (tree-prior) with 10 groups [154]. To calibrate the clock, an uncorrelated lognormally distributed relaxed clock model [155] was used to allow for rate variation among lineages. An exponentially distributed prior with mean 5×10^{-7} s/s/y was placed on the mean clock rate. To allow for uncertainty in the sampling dates of ancient genomes, uniform priors across the date range defined by radiocarbon dating were placed on their ages (Figures S6I–S6L). Default priors were used for all other model components. To confirm clock-like evolution we performed a Bayesian date randomization test [81, 150, 151] (DRT) by permuting sampling dates across genomes and repeating the analysis. We performed 50 replicates and assessed significance by comparing the molecular clock rate estimates of the replicates to those estimated under the true sampling dates. As in the permutation test for the root-to-tip regression analysis above, we fixed the sampling dates of ancient genomes to the middle of the date range defined by radiocarbon dating.

MCMC chains were run for 50 million steps and parameters and trees sampled every 5000 steps. Convergence was assessed in Tracer v.1.7 [113] after discarding 30% of the chains as burn-in and Treeannotator [82] was used to compute MCC trees of the resulting posterior tree distributions. Results were visualized in Rstudio [106] using ggplots2 [104, 105], ggtree [114] and custom scripts.

Robustness of molecular clock dating

To test the robustness of the molecular clock dating results, we repeated the analyses using different combinations of demographic (constant population size coalescent, exponential growth coalescent, Bayesian skyline plot with 10 groups) and clock (strict and relaxed) models. Default priors were used for all demographic models. The same prior was used for the strict clock rate as for the mean clock rate in analyses with a relaxed clock model (exponential distribution with mean 5×10^{-7}s/s/y). Furthermore, to test the effect of constraining the sampling dates of ancient genomes to the date ranges defined by radiocarbon dating (referred henceforth as narrow uniform priors), we repeated all analyses using wide uniform priors between 1000 CE and 2000 CE).

The demographic model had little effect on the estimated molecular clock rate, divergence times and sampling dates as seen in the graphics (Figure S6). Nonetheless, a constant effective population size leads to slightly older divergence date estimates. The demographic models tested represent very different scenarios (constant effective population size, exponential growth and flexible growth and decline). Since all three models give similar estimates, we are confident that our results are robust to the choice of demographic model.

Estimates under different clock models are largely overlapping. A relaxed clock model leads to wider HPD intervals than a strict clock and thus represents a more conservative choice. Furthermore, the HPD interval of the coefficient of variation (of the clock rate) estimated under a relaxed clock model does not include 0, indicating strong evidence for rate variation among lineages.

Relaxing the constraints on the sampling dates of ancient genomes leads to more recent divergence time estimates more in line with previous analyses [41] and a faster clock rate estimate that is similar to the rate reported by Beale et al. for TPA [8]. Similarly, the sampling date estimates of the ancient TPE genomes are more recent. Nevertheless, posterior distributions of the sampling dates of all ancient genomes except CHS119 place considerable weight on the date range defined by radiocarbon dating, with median estimates either included in the radiocarbon date range (SJ219 and 133) or slightly earlier (PD28) (as seen in Figures S6I–S6L).

Virulence analysis

Virulence factors (details: see below) represented by the four ancient European genomes were assessed through a gene presence/absence analysis as described by Andrades Valtueña et al. [156]. For sanger-sequenced modern genomes used as comparison (Chicago, Mexico A, Sea81-4, SS14), we used artificial, 100nt long reads simulated with the tool Genome2Reads (integrated in the EAGER-pipeline [69]) to facilitate mapping them in a concise manner with all other, NGS-sequenced data. A set of 60 sequences previously associated with putative virulence functions [52, 87, 88, 157] were examined based on the annotated Nichols reference genome (GenBank CP004010.2) [75] with a preliminary quality filtering threshold of 37 and without a quality filtering. The resulting effect of 0-quality filtering is that all reads are allowed to map, despite the presence of duplicated regions (in the *tpr* gene paralogs in particular) whereas quality filtering with a threshold set to larger than 0 omits all reads mapping to identical regions, making the coverage of these regions appear extremely low. The coverage over each gene was calculated using genomeCoverageBed in BEDTools version 2.250 [103] (Table S3). The heatmap visualization of the gene-by-gene coverage of reads was created using ggplot2 package in R [104, 105] (Figure 4).

QUANTIFICATION AND STATISTICAL ANALYSIS

In silico screening

In total, nine samples were screened for the presence of *T. pallidum*. The candidates for further capture methods and genomic analyses were selected according to threshold values as indicated above (see Read processing, mapping and variant calling in METHOD DETAILS).

Phylogenetic analysis

Phylogenetic analyses were performed with the ML algorithm in RAxML v. 8.2.12 [111] (see Read processing, mapping and variant calling in METHOD DETAILS), with the rapid bootstrap algorithm. Positions having > 25% missing data or identified as well as recombining and mapping-obstructing genes (as defined in) were excluded from the nucleotide alignment prior to the analysis.

Molecular clock test

The robustness of the molecular clock dating was conducted by repetitions of different combinations of demographic and clock models in BEAST2 v.2.6 [82]. To confirm clock-like evolution a Bayesian date randomization test (DRT) was used by permuting sampling dates across genomes and repeating the analysis. To test the effect of constraining the sampling dates of ancient genomes to the date ranges defined by radiocarbon dating, we repeated all analyses using wide uniform priors between 1000 CE and 2000 CE. (see Figures S5 and S6 and Molecular clock dating in METHOD DETAILS above).

Dating analysis

Dating analysis was performed with BEAST2 v.2.6 [158] as indicated above (see Molecular clock dating in METHOD DETAILS). MCMC chains were run for 50 million steps, with parameters and trees sampled every 5000 steps.